Green Synthesis and Characterization of Ag/Zn Bimetallic Nanoparticles Using Garlic (*Allium Sativum L*) Plant Extracts for Antibacterial Applications

Efa Kebeda Balcha

A Thesis Submitted to Department of Applied Chemistry
School of Applied Natural Science

Presented in Partial Fulfillment of the Requirements for the Master of Science Degree in Applied Chemistry (Inorganic chemistry)

Office of Post Graduate Studies
Adama Science and Technology University

September, 2021
Adama, Ethiopia

Green Synthesis and Characterization of Ag/Zn Bimetallic Nanoparticles Using Garlic (*Allium Sativum L*) Plant Extracts for Antibacterial Applications

Efa Kebeda Balcha

Advisor: Tegene Desalegn (Ph.D.)

Co-Advisor: H.C Ananda Murthy (Ph.D.)

A Thesis Submitted to Department of Applied Chemistry,
School of Applied Natural Science

Presented in Partial Fulfillment of the Requirements for the Master of Science Degree in Inorganic chemistry

Office of Post Graduate Studies
Adama Science and Technology University

September, 2021
Adama, Ethiopia

Approval Page

We, the advisors of the thesis entitled "**Green Synthesis and Characterization of Ag/Zn Bimetallic Nanoparticles Using Garlic (*Allium Sativum L*) Plant Extracts for Antibacterial Applications"** and developed by **Efa Kebeda Balcha**, hereby certify that the recommendation and suggestions made by the board of examiners are appropriately incorporated into the final version of the thesis.

____________________	__________	__________
Major Advisor	Signature	Date
____________________	__________	__________
Co-advisor	Signature	Date

We, the undersigned, members of the Board of Examiners of the thesis by **Efa Kebeda Balcha** have read and evaluated the thesis entitled "**Green Synthesis and Characterization of Ag/Zn Bimetallic Nanoparticles Using Garlic (*Allium Sativum L*) Plant Extracts for Antibacterial Applications**" and examined the candidate during the open defense. This is, therefore, to certify that the thesis is accepted for partial fulfillment of the requirement of the degree of Master of Science in Inorganic chemistry.

____________________	__________	__________
Chairperson	Signature	Date
____________________	__________	__________
Internal Examiner	Signature	Date
____________________	__________	__________
External Examiner	Signature	Date

Finally, approval and acceptance of the thesis is contingent upon submission of its final copy to the Office of Postgraduate Studies (OPGS) through the Department Graduate Council (DGC) and School Graduate Committee (SGC).

____________________	__________	__________
Department Head	Signature	Date
____________________	__________	__________
School Dean	Signature	Date
____________________	__________	__________
Office of Postgraduate Studies, Dean	Signature	Date

Declaration

I hereby declare that the MSc Thesis report entitles "**Green Synthesis and Characterization of Ag/Zn Bimetallic Nanoparticles Using Garlic (*Allium Sativum L*) Plant Extracts for Antibacterial Applications"** is my original work and has not been presented for a degree in any other university and all sources of material used for this thesis have been duly acknowledged.

Efa Kebeda Balcha ______________ ______________

Name of the Student Signature Date

Recommendation

We, the advisors of this thesis, hereby certify that we have read the revised version of the thesis entitled "**Green Synthesis and Characterization of Ag/Zn Bimetallic Nanoparticles Using Garlic (*Allium Sativum L*) Plant Extracts for Antibacterial Applications"** prepared under our guidance to **Efa Kebeda Balcha** submitted in partial fulfillment of the requirements for the degree of Mater's of Science in Inorganic chemistry. Therefore, we recommend the submission of the revised version of the thesis to the department following the applicable procedures.

______________________	____________	____________
Major advisor	Signature	Date
______________________	____________	____________
Co-advisor	Signature	Date

Acknowledgement

First of all, I thank Almighty God for being with me in all aspects of my works. He has always been with me, led my path and helped me to achieve my goals.

Conducting this thesis research could not be fruitful without the generous help of individuals. In particular, I have to express my deepest gratitude to my advisor, Dr. Tegene Desalegn who helped me with continuous guidance and encouragement in all aspects of this work. Next, the greatest thanks go to my co-advisor Dr. H.C. Ananda Murthy who properly guided me and contributing ideas as well as sharing of his precious time to read and comment on this research thesis. Also, I would like to give my honorable thanks to Adama Science and Technology University, the school of applied natural science, department of applied chemistry as a whole for giving me a scholarship opportunity.

I would also like to thank the Department of Applied Biology for allowing me to use UV-Vis Spectroscopy and conduct Antibacterial Activity Applications, the Department of Materials Science Engineering for allowing me to use XRD instruments, and Addis Ababa University College of Natural Science for running FTIR spectral analysis.

My thanks also extend to my families, friends and colleagues for their encouragement, help and comments given in proceeding of my work. I love all of you!

TABLE OF CONTENTS

LIST OF TABLES

LIST OF FIGURES

LIST OF ACRONYMS

ASTU--------------------------Adama Science and Technology University

BMNPs----------------------------Bimetallic Nanoparticles

FTIR------------------------------Fourier Transform Infrared Spectroscopy

FWHM -------------------------Full Width at Half Maximum

IR ---------------------------------Infrared

MMNPs ------------------------Monometallic Nanoparticles

MRI ----------------------------Magnetic Resonance Imaging

NADH --------------------------Nicotinamide Adenine Dinucleotide

NPs------------------------------Nanoparticles

PVP------------------------------Poly Vinyl Pyrrolidone

SEM------------------------------Scanning Electron Microscope

SPR -----------------------------Surface Plasmon Resonance

UV-Vis---------------------------Ultraviolet-Visible Spectroscopy

XRD-------------------------------X-Ray Diffraction

ZOI--------------------------------Zone of Inhibition

ABSTRACT

In this study, Ag/Zn bimetallic nanoparticles (BMNPs) and silver nanoparticles (Ag NPs) were synthesized via the green synthetic method by using the extracts of Allium Sativum L plant. The antibacterial activities of Ag/Zn bimetallic and Ag NPs were investigated against selected bacterial strains. The synthesized NPs were characterized by using techniques such as X-ray diffraction (XRD), scanning electron microscopy (SEM), Fourier transform Infra-red (FTIR) and UV-vis spectroscopy. The XRD results confirmed cubic crystal structure for the Ag/Zn BMNPs and the average crystallite size was found to be 17.47 nm. Ag NPs were also found to exhibit cubic phase structure and an average crystallite size of 9.31 nm. UV-vis spectra of Ag NPs and Ag/Zn BMNPs showed absorbance maxima at 402 nm and 360 nm, respectively. The SEM images showed a spherical shape for Ag NPs and Ag/Zn BMNPs. The antibacterial activities of the synthesized nanoparticles were tested against gram-negative bacterial strains (Escherichia coli and Pseudomonas aeruginosa) and gram-positive bacterial strains (Streptococcus pyogenes and Staphylococcus aureus) using the agar-well diffusion method. The maximum zones of inhibition of 19 mm and 16.5 mm were recorded for Ag NPs and Ag/Zn BMNPs against P. aeruginosa, respectively. In addition, the antibacterial effect was found to increase with an increase in the concentration of both Ag and Ag/Zn NPs. The results substantiated that the antibacterial activity of Ag NPs was superior to that of Ag/Zn BMNPs for both gram-negative and gram-positive bacterial strains.

Key words: *Ag NPs, Ag/Zn bimetallic NPs, Green synthesis, Allium Sativum L plant Antibacterial activity.*

1. INTRODUCTION

1.1. Background of the Study

Nano science and nanotechnology have grown at an enormous rate in the last three decades, and recent advances in nanostructured materials have opened up new opportunities for diverse applications in electronics, catalysis, energy, materials chemistry, and even biology (Bang, J. & Suslick, K., 2010). Materials in the nanometer-size regime often exhibit properties distinct from their bulk counterparts, in part because nano-sized clusters have electronic structures that have a high density of states, but not yet continuous bands (Dehghan Banadaki & Kajbafvala, 2014). Nanoparticles (NPs) are a special class of organic or inorganic materials having a size in the range of 1 to 100 nm in at least one dimension. NPs have unique and enhanced functional properties such as a high surface area to volume ratio and more atoms on their surface than their micro-or macro-scale counterparts owing to their nanoscale feature (Khatami *et al*., 2018). An increase in solid solubility of alloy components with decreasing particle size is one of the prominent effects (Shah *et al*., 2012).

Bimetallic nanoparticles (BMNPs), composed of two distinct metal elements, have a certain mixing pattern or chemistry sequence and geometry architecture and perform specific functions (Duan & Wang, 2013). Their performance often surpasses the enhancement of the properties associated with their single counterparts and exhibits many interesting and useful properties with broadened application fields often explained by synergistic effects of nanomaterial. By changing their components and morphologies, their relevant physical, electrical, or chemical performances can be successfully modified. The structures of bimetallic nanoparticles are complicated and can take multiple forms. According to the mixing pattern of two different metals, three main types of structures can be identified for bimetallic nanoparticles, that is, core/shell, hetero-structure or intermetallic, and alloyed structures. In the formation process of core/shell structures, often one type of metal ions is reduced first and forms an inner core, while the other metal grows as a shell surrounding the nucleated core. However, under proper conditions, individual nucleation and growth of two kinds of metal atoms can occur. If they share a mixed interface during the growth process, hetero-structure forms. Intermetallic and alloys belong to another group entirely different from core/shell or hetero-structure bimetallic nanoparticles (Dehghan Banadaki & Kajbafvala, 2014).

BMNPs are the complex combination of two different metal constituents in nanoscale. When two metals are combined, it can show not only the properties of its constituents but also new and enhanced properties derived by the synergy of the combination. A bimetallic system is a complex system consisting of two metal components. The characteristics of a bimetallic surface bond can be altogether distinct from the respective 3-D alloy bond. This marks the reason for their wide technological applications in areas of catalysis, electrochemistry, metallurgy, and microelectronics fabrication. The catalytic ability of a bimetallic particle is firmly confided in its nanoparticle size, structural organization, and composition. So it is essential to choose the suitable methodology and experimental conditions to prepare bimetallic nanoparticles with the desired morphology and properties that are appropriate to the application (Rodriguez *et al*., 1992).

BMNPs have many applications in various disciplines has expanded considerably. They possess unique physical properties and high reactivity with high surface to volume ratio. An attempt has been made to determine the antimicrobial activity of zinc and silver nanoparticles; also the antimicrobial activity of Ag/Zn bimetallic nanoparticles is determined. It is found that the antimicrobial activity increases when the bimetallic nanoparticles are used (Nazeruddin et al., 2014).

BMNPs have excellent properties compared to monometallic nano-crystals owing to their improved electronic, optical and catalytic performances. BMNPs often improve the selectivity of metal-catalyzed reactions (Shah *et al*., 2012). Moreover, the change in the composition of metals provides another dimension in tailoring the properties of BMNPs besides the usual size and shape manipulation (Su & Wang, 2013). BMNPS may have random, core-shell and alloy structures. In a random structure, atoms are arranged haphazardly. One element in cluster-in-cluster type forms nano clusters and the other acts as a binder. In bulk metals, two kinds of metal elements often provide an alloy structure (Zaleska-Medynska *et al*., 2016). Elements with similar atomic sizes form a random alloy while the intermetallic alloy is formed by elements of different atomic sizes (Shah *et al*., 2012). Silver-gold, silver-copper, copper-nickel and iron-nickels are some examples of BMNPs reported in the recent past (Li *et al*., 2006).

1.2. Statement of the Problem

Recently, researches also have been focused to diversify the application of metallic nanoparticles in areas such as antibacterial activities. Huge literature reports are indicating that antibacterial and antifungal drugs methods of synthesis are posing serious impacts on the environment and human health. There were also reports of increased drug resistance by the bacterial strains. So, searching for safe and effective antibacterial agents for therapeutic and non-therapeutic purposes has been continuously encouraged. The chemical method of synthesizing nano particles is extremely expensive and also involves the use of toxic, hazardous chemicals, which pose potential environmental and biological risks. The biosynthesis process is used where plants extracts are used for the fabrication of nanoparticles being chosen as it is relatively rapid, low cost, eco-friendly. However, there were few reports on the synthesis and application of BMNPs. Hence, in this research Ag/Zn BMNPs and Ag NPs were planned to be synthesized using garlic (*Allium Sativum L*) plant extract, the resulting mono and bimetallic nanoparticles were characterized and finally, their antibacterial application has been evaluated.

1.3. Objectives

1.3.1. General Objective

The main objective of this research is to synthesis and characterizes Ag/Zn BMNPs using *Allium sativum L* plant extract and study their antibacterial activities.

1.3.2. Specific Objective

The specific objectives of this research work are;

- ✓ To synthesize Ag NPs and Ag/Zn BMNPs from respective salts of both metals using the extract of *Allium sativum L* plant.
- ✓ To characterize the synthesized Ag NPs and Ag/Zn BMNPs using UV-vis, XRD, SEM and FTIR techniques.

- ✓ To investigate the antibacterial activity performance of the synthesized Ag NPs and Ag/Zn BMNPs against *E. coli, P. aeruginosa, S. pyogenes* and *S.aureus*.

1.4. Significance of the Study

Infectious diseases are one of the leading causes of death of children, adolescents and olds. The development of alarming resistance of bacteria towards antibacterial agents is a major global public health problem. Thus, we need to have effective alternate antimicrobials to combat such resistant bugs. The results of this study could be used as a source of information for the scientific community about the green synthesis of bimetallic nanoparticles and helps to use Ag/Zn BMNPs as antibacterial agents. The data reported could be a base for researchers interested to work to carry further studies in areas of BMNPs.

2. LITERATURE REVIEW

2.1. Nano Science and Nano Technology

Nano science is the study of phenomena and manipulation of materials at atomic, molecular and micro molecular levels, where properties differ significantly from those at a larger scale whereas nanotechnology is the design, creation, characterization, exploitation and utilization of structures, devices and systems by controlling shape and size at the nanometer scale. In other words, nanotechnology deals with the engineering of functional systems and applications of nanoscale materials that have the size and structural features lay between those of atoms and their bulk materials, new properties and functions. (Gude *et al*., 2016), (Mandal *et al*., 2006).

Nanotechnology speaks to the plan, creation and use of materials at atomic, molecular and macromolecular levels, keeping in mind the end goal to deliver new nano-sized materials. As of late, the meeting of nanometer size scale advancements and biological techniques has paved the way for the new field of nano biotechnology (Mazhar *et al*., 2017). It is generally centered on the creation, control, and utilization of materials at the nanometer-scale for cutting-edge biotechnology (Zaib & Iqbal, 2019).

Nanotechnology is the science and technology of small things–in particular, things that are less than 100nm in size. One nanometer is 10^{-9} meters or about 3 atoms long. For comparison, human hair is about 60-80,000 nm wide. Scientists have discovered that materials at small dimensions such as small particles, thin films, etc., can have significantly different properties than the same materials at a larger scale. Nanostructured objects with nanometer scale features are not new and they were not first created by man. There are many examples of nanostructures in nature in the way that plants and animals have evolved. Similarly, there are many natural nano-scale materials, such as catalysts, porous materials, certain minerals, soot particles, etc., that have unique properties particularly because of the nano-scale features (Bhatt & Gupta, 2018). In the past decade, innovations in our understanding of nanotechnology have enabled us to begin to understand and control these structures and properties to make new functional materials and devices (Khatami *et al*., 2018).

2.2. Nanoparticles (NPs)

Nanoparticles are particles in the nano scale size between 1nm and 100nm with a surrounding interfacial layer. They are very small particles with improved thermal conductivity, catalytic reactivity, nonlinear optical performance, and chemical stability due to their larger surface area–to–volume ratio. The interfacial layer is an integral part of nano scale matter, fundamentally affecting all of its properties (Jassal, 2020). In nanotechnology, a particle is defined as a small object that behaves as a whole unit concerning its transport and properties. NPs are the great scientific interest as they are, in effect a bridge between bulk material and atomic or molecular structure. A bulk material should have constant physical properties regardless of its size, but at the nano scale, size-dependent properties are often observed (Nadaroglu *et al*., 2017).

2.2.1. Types of Nanoparticles

Nanoparticles are of several types and can be classified based on: origin, dimension, and structural organization (Mazhar *et al*., 2017). Based on origin, natural nanoparticles are nanoparticles that belong to natural resources are called natural nanoparticles such as viruses, protein, antibodies, etc. Artificial nanoparticles are those nanoparticles that are intentionally prepared for a purpose following the proper manufacturing process and required techniques are called artificial nanoparticles such as carbon nanotubes, metal nanoparticles, nano membranes, etc. Based on the dimension, zero-dimensional (0-D) are those nanoparticles that hold a critical range of 1-100 nm in all three directions of space vectors are zero-dimensional nanoparticles (Figure 2.1). Quantum dots and metal nanoparticles are perfect examples of zero-dimensional nanoparticles (Mazhar *et al*., 2017).

Most of these particles are spherical or may be cubic, polygonal or clusters. As the name suggests in one dimensional (1-D), one dimension of the nanostructure is outside the nanometer range and two spatial vectors are committed to critical length scale thereby allowing growth only in the third direction. Example: nanowires, nano rods, etc. These nanomaterials are usually long but with a small diameter. Two dimensional (2-D) nanoparticles have two dimensions of the nanostructure outside the nanometer range and only one vector is committed to critical length scale hence allowing growth in two spatial directions. Example: Nano films, nano sheets, nano walls, etc. The surface of these films can be several micrometers square but thickness would be in the nano range only. Three-dimensional (3D) nanoparticles have all three dimensions are outside the nano scale range. These include bulk materials like fullerene (Mazhar *et al*., 2017).

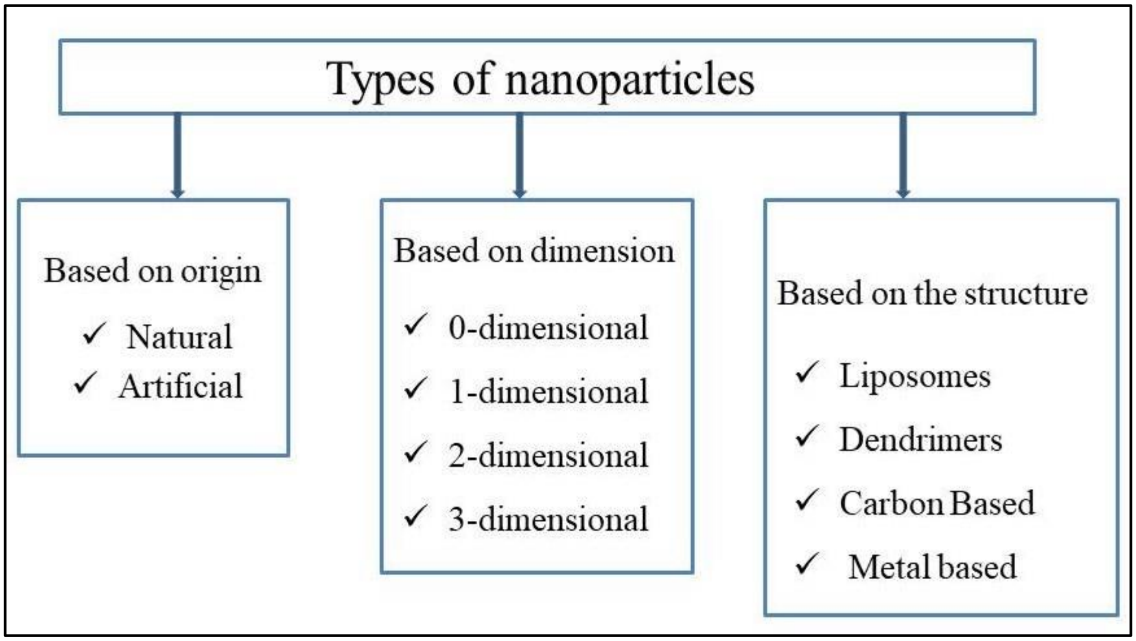

Figure 2.1: Flowchart representing Types of Nanoparticles (Mazhar *et al*., 2017)

Based on the structural configuration some liposomes are bi-layered concentric vesicles composed of natural or synthetic phospholipids. Liposomes can alter the pharmacokinetic profile of drug-loaded. Dendrimers are polymers with Nano dimensions and controlled structure. Dendrimers are widely used for targeted drug delivery. Carbon-based material has hollow cage-like architecture, which includes carbon nanotubes and fullerene. Small dimensions of carbon nanotubes along with excellent electrical, mechanical and physical properties make them very unique. Fullerenes resemble certain bioactive molecules with similar dimensions and therefore have potential applications in medicines. Metal-based, as the name suggests, have metal as a component of these particles. They can be in the form of nano shells or closely packed semiconductors like quantum dots. Depending on the number of constituent particles metal NPs can be classified as, monometallic, bimetallic (composed of two metals), trimetallic (containing three metals), or multimetallic NPs (containing more than three metals) (Mazhar *et al*., 2017).

2.3. Monometallic nanoparticles (MMNPs)

Monometallic nanoparticles (MMNPs) consist of only single metal. The constituted metal atom determines the properties of these nanoparticles**.** MMNPs are of different types depending upon the type of metal atom present such as magnetic, metallic and transition metal nanoparticles, etc. They can be prepared by different routes but the most important is the chemical method. Their structure can be stabilized using various functional groups. A greater interest in the field of metallic nanoparticles was observed in the last few decades due to their enhanced physical and chemical properties. For this reason, they are used for several applications such as in electronic, optical and catalysis, etc. In addition, they have also been used as antimicrobial agents against several microorganisms and anti-cancer activity (Chauhan *et al*., 2019).

2.3.1. Synthesis of Silver Nanoparticles

Silver nanoparticles (Ag NPs) are nontoxic and have a high electrical and thermal conductivity and strong oxidation properties but the hindrance to its use in commercial products is of high cost. Mono dispersed colloidal solution of silver nanoparticles is generally synthesized by chemical reduction electrochemical, photochemical and sonochemical methods (Figure 2.2) and also using a pulsed laser (Tran *et al*., 2018).

2.3.1.1. Synthesis Methods of Silver Nanoparticles

Recently, many techniques have been used for the synthesis of Ag NPs by using chemical, physical, and biological methods. Each method has its pros and cons with common problems of cost, scalability, uniform particle size, and size distribution. Traditionally, metal nanoparticles are produced by physical methods like ion sputtering or pulsed laser ablation and chemical methods such as reduction, hydrothermal, sol-gel methods, and so on. However, recently, environmentally friendly synthesis methods (by using natural products) have been developed under the branch of "green syntheses." Depending upon the selected path of synthesis and different experimental conditions, the silver NPs of different morphology, sizes, and shapes can be obtained. Nevertheless, the most important criteria are the size distribution that should be achieved as narrow as possible for the target-specific applications (Tian *et al*., 2019).

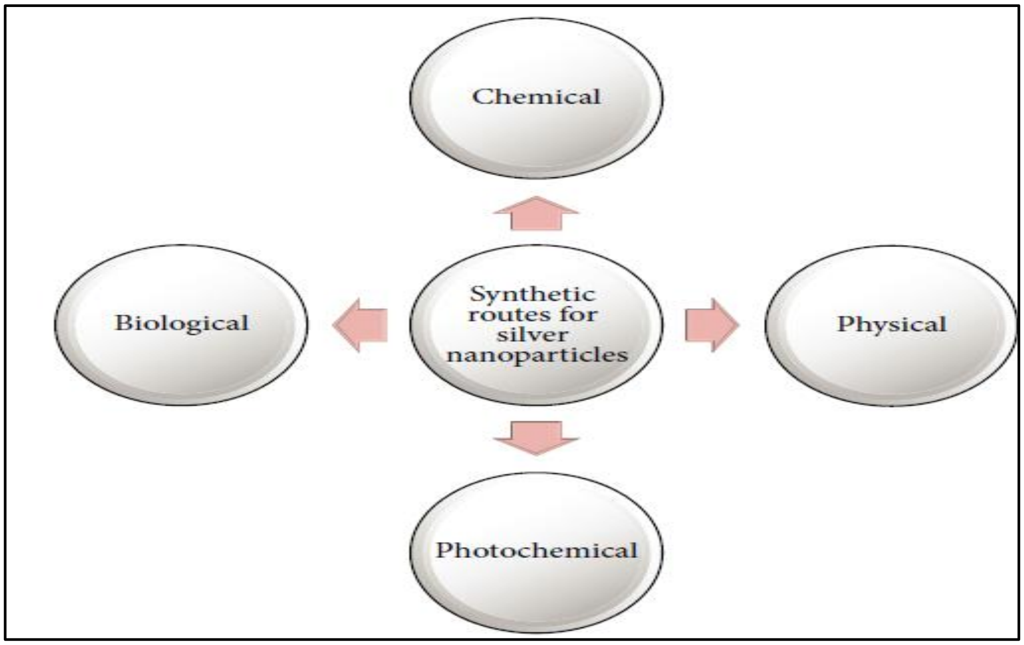

Figure 2.2: Various synthetic routes adopted for the synthesis of Ag NPs with uniform geometry (Haider & Kang, 2015)

Chemical Method: Among the reported methods, so far, chemical methods are preferred for the preparation of Ag NPs due to the ease of synthesizing them in solution. Many research groups are using these methods to synthesize Ag NPs in various sizes and shapes. For example, one research group synthesized monodisperse silver nanocubes by simply reducing $AgNO_3$ with ethylene glycol in the presence of poly vinyl pyrrolidone (PVP) polymer. The process was called the polyol process. In this process, it has been revealed that ethylene glycol works as both the solvent and the reducing agent. Furthermore, the size and shape of the nanocubes were dependent on the molar ratio of $AgNO_3$ and PVP (Khatami *et al*., 2018).

In another reported method, mono dispersed Ag NPs were synthesized using $AgNO_3$, oleylamine, and liquid paraffin. Oleylamineparaffin system was used for controlling high temperature which paid a pivotal role in determining the particle size of the synthesized Ag NPs. Liquid paraffin was used to sustained high temperatures and secondly helped in avoiding the use of solvents that would hamper the whole synthetic process. Normally, the synthesis of Ag NPs by chemical method banks on three factors stages: Ag precursor, reducing agents, and stabilizing agent (Haider & Kang, 2015)

Physical Method: Along with the chemical methods used, various alternative techniques were also adopted by researchers for the synthesis of Ag NPs. Usually in those techniques, evaporation and condensation processes are implemented for the synthesis of Ag NPs. Similar to a chemical method, and these methods have their own merits and demerits. One of the most common drawbacks of these methods is the higher energy requirement and time-consuming. Therefore, researchers have reported numerous alternative physical methods for the synthesis of Ag NPs instead of implementing conventional condensation and evaporation methods. These methods not only reduced the preparation time but also are energy-friendly. For example, the thermal-decomposition method was implemented for the synthesis of Ag NPs in solid form. In such a method, a complexation reaction between Ag and oleate at elevated temperature was carried out for the synthesis of Ag NPs with particle size less than 10 nm (Sintubin *et al*., 2012).

Photochemical Synthesis: In the photochemical techniques mainly two different methodologies are implemented for the synthesis of Ag NPs: photo-physical and photochemical techniques. In photochemical techniques, Ag NPs are synthesized by photo-reduction of precursor or Ag ions using photo-chemically activated intermediates such as radicals. In one of the methods, Ag NPs were synthesized using UV radiation and an aqueous solution that acts as a stabilizing agent. The surfactant used in the study helped in maintaining the stability, mono dispersion, and uniform size of the synthesized Ag NPs (Haider & Kang, 2015).

Biological Synthesis: In biological methods, Ag NPs are synthesized using plants (such as algae, yeast, fungi, and bacteria) as reducing and stabilizing agents. For example, in one study the leave *Shewanella oneidensis* (a metal reducing agent) was used for the biosynthesis of Ag NPs using $AgNO_3$ solution as a precursor. The synthesized Ag NPs size was less than 15 nm, with uniform dispersion, spherical shape, enhanced stability, and large surface area. Such methods used for the synthesis of Ag NPs are highly economical and reproducible and consume lesser energy contrary to the conventional methods (Prem Nawaz *et al*., 2018).

In another study, *Trichoderma viride* fungus was used for the biosynthesis of Ag NPs from $AgNO_3$ precursors. Furthermore, stable Ag NPs with a size of less than 20 nm were synthesized by using airborne bacteria (*Bacillus sp*ecies) using $AgNO_3$ as the precursor. The biosynthesized Ag NPs were collected from the periplasmic region (space between the outer and inner membrane) of the bacterial cell. NPs can also be synthesized from *Cadaba Fruticosa* leaves using $AgNO_3$ as the precursor. The biologically synthesized nanoparticles were very potent against microbes (Chalie u *et al*., 2019).

2.3.2. Application of Ag NPs

In recent years, metal NPs have attracted much attention owing to their excellent high activity against many species of bacteria and fungi. These metal nanoparticles revealed the new optical, electrical, and mechanical properties and higher reactivity due to their high surface-to-volume ratio, distinct from those of the corresponding metallic bulk materials. The application of nanoscale materials and structures is an emerging area of nanoscience and nanotechnology. Nano-sized metal particles have been used widely in various fields including catalysis and photonics. Among various metals, silver nanoparticles (Ag NPs) are of particular interest due to their remarkable antimicrobial and localized surface plasmon resonance properties. They have unique optical, electrical, and thermal properties and are incorporated into the industrial application of electronics, catalysis, and photonics. In recent years, with a higher integrated density of electronic components, there are growing demands for the thickness or the width of printed electronic circuits due to considering the space between these circuits. Therefore, the synthesis of Ag NPs becomes an important issue in the electronic industry (Natsuki *et al*., 2015).

2.4. Bimetallic Nanoparticles (BMNPs)

BMNPs composed of two different metals have drawn a greater interest than monometallic nanoparticles from both scientific as well as technological points of view. Constituting metals and their nanometric size determine the properties of the bimetallic nanoparticles. These are synthesized by the combination of different architectures of metallic nanoparticles. They offer us the tendency of optimizing the energy of the plasmon absorption band of metallic mixture which offers us a multipurpose tool for bio-sensing. These properties may differ from those of pure elemental particles and include unique size-dependent optical, electronic, thermal and catalytic effects (Chauhan *et al*., 2019). Different methods have been proposed for their preparation and detailed characterization. These days' researchers are focusing on selectively preparing new bimetallic nanoparticles in different forms, such as alloys, core-shell and contact aggregate. Actually, through bi-metallization, the catalytic properties of the resulting nanoparticles can be improved to a great extent which may not be achievable by the use of monometallic catalysts. In bimetallic catalysts, the electronic effect plays an important role which describes the charge transfer. Alloying of the constituting elements can result in the structural changes of the bimetallic nanoparticles. From monometallic to bimetallic nanoparticles, an extra degree of freedom is introduced (Sharma *et al*., 2019).

BMNPs are synthesized by a combination of two metal nanoparticles with several architectures (Mazhar *et al*., 2017) as described in Figure 2.3,

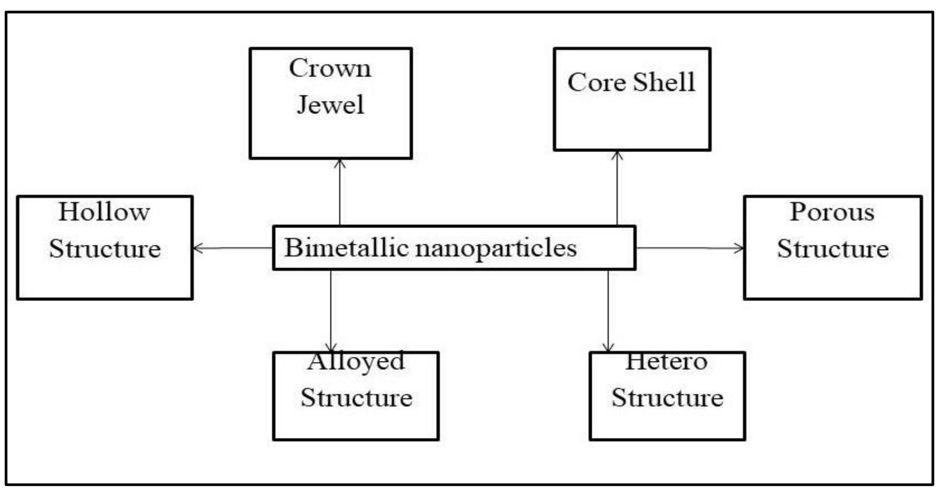

Figure 2.3: Schematics of Bimetallic Nanoparticle Types (Mazhar *et al*., 2017)

a) Crown Jewel Structure: In this type of architecture, one metal atom (jewel atom) is mustered on the surface of other metals in a controlled manner. The 'jewel' metal is usually a costly one with catalytic properties, e.g.: Au, Ag, Pt
b) Hollow Structure: Possess large pore volume and high surface-to-volume ratio. Hold utility in nonreactor.

c) Hetero Structure: One metal forms branches over the Nanocrystalline form of the other.
d) Core-Shell Structure: It's a simple arrangement where an active metal shell is supported on another metal present as a core. Core-shell bimetallic nanoparticles are emerging as propitious catalysts with good efficiency.
e) Alloyed Structure: Bimetallic alloys are formed when two different metal atoms possess homogenous distribution in a single particle.
f) Porous Structure: These are bimetallic alloys with increased surface area, low density and high gas permeability, thereby proving to be better catalysts than their solid counterparts.

2.4.1. Synthesis of BMNPs

Bimetallic nanoparticles can be synthesized through the subsequent or simultaneous reduction of respective metal salts in a variety of ways; in solution. Generally, the synthesis can be done through physical methods, chemical methods and biological methods (Netoa *et al*., 2013). The top-down synthesis approach was a suitable precursor material that is fragmented to nano level in general through physical or chemical means. The physical methods are normally high expensive and enormous energy-consuming to maintain extreme reaction conditions, as well as having lower production rates. while, the high yield, low-cost chemical methodologies are utilizing various chemicals to achieve reduction and to prevent agglomeration, are having constraints of harmful solvents, the toxicity of the precursor chemicals, and the release of more toxic by-products (Huynh *et al*., 2020).

Thus there is a need for a new green eco-friendly approach of synthesizing metallic nanoparticles by biological means via bacteria, fungi and plants to develop nontoxic, high yield, low-cost procedures. This biogenic metallic nanoparticle synthesis can be through two mechanisms, either through bio-reduction, where metal ions get biologically reduced to stable forms, or by biosorption, where metal ions get bonded to the organism then get converted to stable nanoparticle forms (Salunke *et al*., 2014).

For example, by using the neam (*Azadirachta indica*) leaf broth for the reduction of a 1:1 M mixture of Au^{3+} and Ag^{+} ions. They reported that bimetallic Au_{core}-Ag_{shell} nanostructures formation as the gold ions have a faster reduction rate than that of silver ions. The reducing sugars and/or terpenoids present in the Neem leaf broth facilitated the reduction of the metal ions to pure metallic and bimetallic nanoparticles. The leaf broth constituents such as flavanone and terpenoids might act as stabilizing agents for the nanoparticles. The silver NPs generated are rather smaller and do not form a uniform layer around the gold nanoparticles. The bimetallic nanoparticles were in the range of 50–100 nm as they tend to aggregate (Thirumurugan, 2010).

The synthesized Au/Pd bimetallic nanoclusters are using a multifunctional peptide ligand. They designed multifunctional peptides that can form Au nanoparticles along with the capability to bind with other metal ions like Pd^{4+} or Pt^{2+}. The Pd^{4+} ions, when exposed to the peptide-decorated Au NPs, binds with it and in the presence of $NaBH_4$, reduces to Pd nanoparticles, which get assembled around the Au core to form a core-shell structure (Slocik & Naik, 2006).

2.5. Synthesis method of BMNPs

The synthesis of NPs involves two major approaches: there are top-down and bottom-up approaches. Top-down synthesis is cutting of bulk material to get nano-sized particles, whereas in bottom-up synthesis atoms build up into new molecules which grow into clusters and then form particles of nano-scale. Since two techniques hold significant differences (Table 2.1), therefore below we discuss a few of them (Sharma *et al*., 2017). Bottom-up and top-down methods are two approaches recommended for the biosynthesis of NPs (Figure 2.4). In the bottom-up approach, the most important reaction that occurred is oxidation/reduction. The synthesis of NPs is currently an important area of research, which seeks an eco-friendly approach and green materials. The major steps involved in the preparation of NPs that have to evaluate from the point of green chemistry are:- the solvent medium used for synthesis, environmental benign reducing agent and the non-toxic materials for stabilization of NPs.

Table 2.1: Differences between Top-Down and Bottom-Up approaches of Nanoparticle Synthesis (Mazhar *et al*., 2017)

Top-Down Approach	**Bottom-Up Approach**
• Starts with bulk solid materials	• Starts with atoms, ions and molecules
• Fragmentation of bulk materials into Nanoscale particles in presence or absence of catalyst by application of external mechanical force	• Atoms, ions and molecules act as building blocks that assemble into Nano scale clusters with atomic or molecular precision
• No specific control over shape and size	• Specific control over shape and size
• Faster than bottom-up	• Comparatively slow
• For large scale industrial productions	• For laboratory purposes
• Processes involved are Ball milling, melt mixing, mechanical grinding, etc.	• Processes involved in bottom-up approaches are chemical precipitation, sol-gel process, and pyrolysis.

The majority of the chemical and physical methods largely depend on organic solvents due to the hydrophobicity of the capping agents used. Synthesis with bio-organisms is compatible with the principle of green chemistry: the reducing agent used an eco-friendly approach and capping agent in reaction. The synthesis of inorganic metal oxide NPs (Figure 2.5) using biological elements has received attention due to their unusual properties (optical, electronic, chemical, etc.) (Kalpana & Devi Rajeswari, 2018).

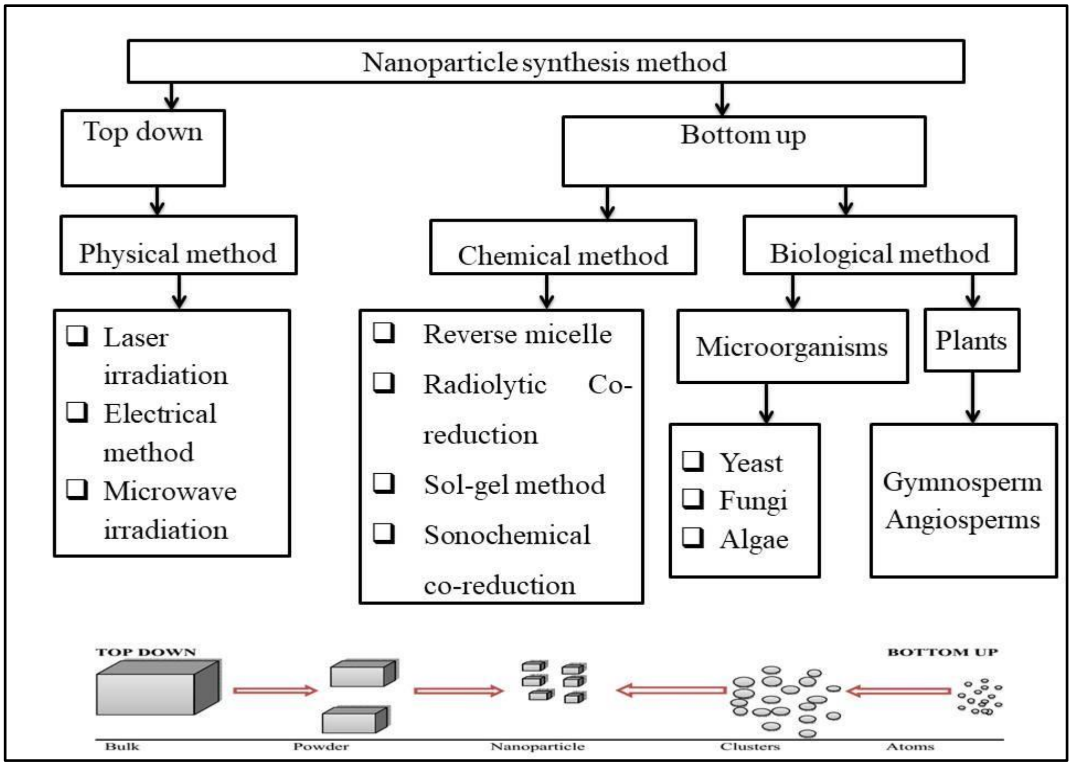

Figure 2.4: General synthesis methods of nanoparticles (Mazhar *et al*., 2017)

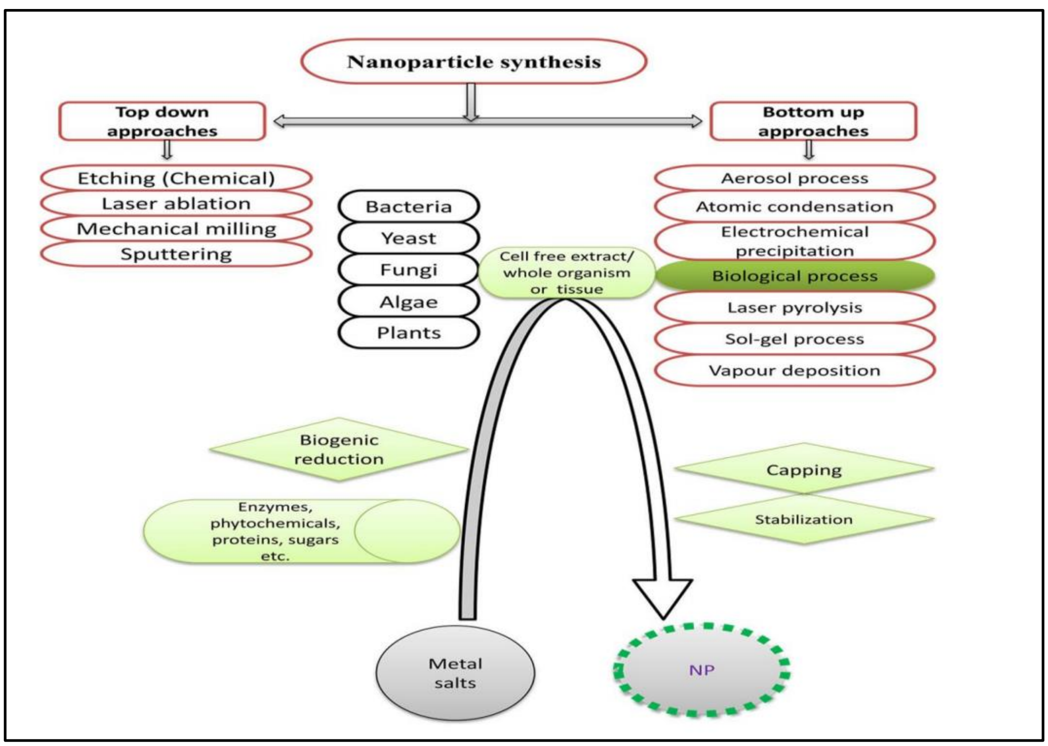

Figure 2.5: Synthesis of nanoparticles from metal salts by different methods (Nadaroglu *et al*., 2017).

Bimetallic nanoparticles (BMNPs) can be synthesized by three different methods. They are: Physical, Chemical and Biological methods.

2.5.1. Physical Method

This method holds certain advantages over chemical methods such as no solvent contamination in prepared film and uniformity in nanoparticle formation. Several physical methods for the synthesis of nanoparticles can be:

Laser Irradiation Method- BMNPs can be synthesized without using any chemical agent and only by laser irradiation of high intensity on an aqueous solution. For Example, Pt/Au BMNPs, Pt and Au are photosensitive therefore in darkroom Pt/Au precursors are prepared by dissolving chloroauric (III) acid tetrahydrate and chloroplatinic (IV) acid hexahydrate in deionized water using the concentration of 0.01% wt irradiating it with laser (Mazhar *et al*., 2017).

Electrical Method- In this process an electrode gap is created by an automatic control system and the procedure is done at this electrode gap and constant current. Particles synthesized are kept in cooling liquid under the effect of gravitational force. For Example, Cu/Ag bimetallic nanoparticles help in the production of water-dispersible copper and copper-silver nanoparticles at room temperature, require an inert atmosphere (Mazhar *et al*., 2017).

Microwave Irradiation- Microwave heating replaces the use of chemicals and reduces reaction time, therefore preferred for bimetallic synthesis. For Example, Fe/Ru bimetallic nanoparticles, ruthenium (III) chloride hydrate ($RuCl_3 \cdot H_2O$) and iron (III) chloride hexahydrate ($FeCl_3 \cdot 6H_2O$) were used to prepare an aqueous solution by adding above two in 1, 2- propanediol. 0.1M ammonia is added drop-wise with continuous stirring. The resulting solution was irradiated using microwave heating giving the dark brown colloidal solution of Fe/Ru bimetallic nanoparticles. Colloidal dispersion is then precipitated by acetone to remove chloride ions and then dried in a vacuum to be redispersed in a mixture of ethanol and water before characterization (Mazhar *et al*., 2017).

2.5.2. Chemical Methods

Advantages of chemical methods over physical methods are that the techniques are not complicated, economic, diverse sizes and shapes can be synthesized, large quantities can be obtained in a short period, doping of foreign atoms during synthesis is possible. Various synthesis methods via chemical route are:

Reverse Micelle Method- Reverse micelles are found in water in oil micro-emulsions with certain compositions as nano-sized droplets. These days they are extensively used in the synthesis of many nano-sized particles. For Example, synthesis of Fe/Co bimetallic nanoparticles, wherein, calcium carbonate is supported by Fe/Co. Carbon nanotubes were prepared by using 5% Fe-Co/$CaCO_3$ by chemical vapor deposition. The reverse micelle technique enables precise control over the size of carbon nanotubes (Wu *et al*., 2001). **Radiolytic Co-Reduction Method**- this method produces highly dispersed as well as uniform-sized metal clusters. Nanoparticles can be synthesized with the use of ionization radiations such as UV, X-Ray as well as Gamma Radiation in presence of a stabilizer only and no other chemicals are required. For example, Ag/Pd BMNPs synthesis was carried out by co-reduction of silver nitrate $AgNO_3$ and ammonium hexachloropalladate (IV) in an aqueous solution (Hai *et al*., 2014).

Sol-Gel Method- The sol-gel method drives from two words; sol and gel. The sol is a stable suspension of colloidal solid particle in liquid. The dispersed phase in sol is so small that there only VanderWaal forces. In gel, the concentration of solid is more than liquid. It is a semi- rigid mass in which the particles or ions left after the evaporation starts to form a continuous network. In most of the gel systems, there exist the covalent interactions. The combination of these two network functions is called sol-gel method. This method mainly consists of two main reactions, hydrolysis and condensation. Various BNPs are synthesized by sol-gel method, such as Au-Ag, Au-Pd and Au-Pt, etc. This method is quite useful because it is a simple, economic and effective method to produce good quality nanoparticles. It is quite interesting since it is a low temperature technique that offers the ability to control the product's chemical composition.(Sharma *et al*., 2019)

Sonochemical Co-Reduction- This method helps in synthesizing NPs of large surface area and small size as compared to other methods. An example of this method is the synthesis of Au/Ru BMNPs. Here Au (III) and Ru (III) ions are sonochemically co-reduced in aqueous solutions using polyethylene glycol as a stabilizer (Huynh *et al*., 2020).

2.5.3. Biological Methods

Several Advantages of biological methods over chemical and physical methods are that the processes are environment friendly, less laborious**,** almost negligible industrial waste and no use of toxic chemicals uses inherent biological methods (Figure 2.6) for NPs fabrication, it is safe and holds various applications that are not possible with physical or chemical synthesis methodologies. Synthesis of NPs via physical and chemical routes is expensive, hazardous and time-consuming. Therefore, there is more focus on nanoparticle synthesis using natural resources such as plants and microbes which are termed green syntheses. Plant-mediated synthesis of nanoparticles is better than microbes mediated as the process doesn't include any synthetic protocols and toxic chemicals as well as has a high reaction rate since the need to grow microbes is eliminated. Biosynthesis of Au-Ag bimetallic alloys from fungal biomass and single-cell protein *Spirulina plantesis* was reported (Mazhar *et al*., 2017)

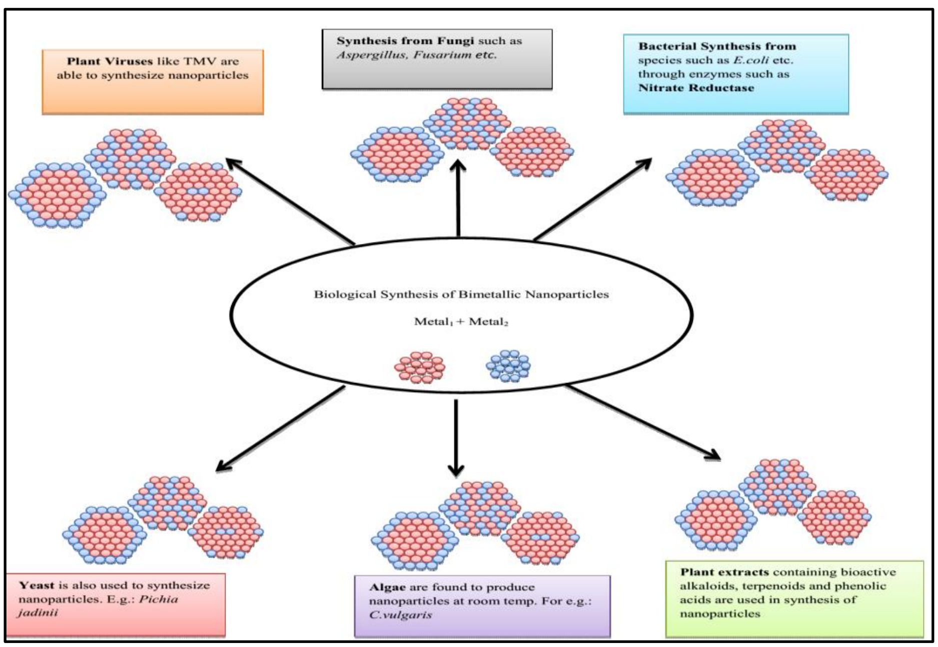

Figure 2.6: Schematic representation of Biological Synthesis of BMNPs with different architectures (Mazhar *et al*., 2017).

2.6. Synthesis of the nanoparticle by using Plants

A slow rate of nanoparticle synthesis using microbes makes plant extracts a preferred choice due to their simplicity, efficiency and viability. Synthesis of NPs using plants is very cost-effective and thus can be used as an economic and valuable alternative for the large-scale production of NPs. BMNPs synthesis process; is initiated by the addition of extracts obtained from plant parts such as leaves, roots and fruits into the aqueous solution of metal ions. The materials present in the plant extract, such as sugar, flavonoid, protein, enzyme, polymer and organic acid, acting as a reducing agent, takes charge in bio induction of metal ions into nanoparticles (Mohamad *et al*., 2013).

In materials science, green synthesis has gained extensive attention as a reliable, sustainable, and eco-friendly protocol for synthesizing a wide range of materials or nanomaterials including metal and metal oxides nanomaterials, hybrid materials, and bio-inspired materials. As such, green synthesis is regarded as an important tool to reduce the destructive effects associated with the traditional methods of synthesis for nanoparticles commonly utilized in laboratories and industry. Green syntheses are required to avoid the production of unwanted or harmful by-products through the build-up of reliable, sustainable, and eco-friendly synthesis procedures. The use of ideal solvent systems and natural resources such as organic systems are essential to achieve this goal (Mohamad *et al*., 2013).

2.6.1. Mechanism of Green Synthesis for Metals and Their Oxide Nanoparticles

Microorganism-based mechanism: There are different mechanisms for the formation of nanoparticles using different microorganisms. First, metal ions are captured on the surface or inside the microbial cells, and then these arrested metal ions are reduced into metal NPs by the action of enzymes. The mechanism of microorganism-assisted silver and gold nanoparticles formed via *Verticillium* species or algal biomass can be shown. First, the silver or gold ions were captured on the surface of fungal cells via electrostatic interactions between ions and negatively charged cell wall enzymes. Then, silver or gold ions were bio-reduced into silver or gold nuclei, which subsequently grew. The two key aspects in the biosynthesis of nanoparticles are NADH (nicotinamide adenine dinucleotide) and NADH-dependent nitrate reductase. Nonetheless, the bio-reduction mechanisms associated with the production of metal salt ions and the resulting metallic nanoparticles formed by microorganisms remain unexplored (Van *et al*., 2020).

Plant leaf extract-based procedures: For nanoparticle synthesis mediated by plant leaf extract, the extract is mixed with metal precursor solutions at different reaction conditions. The parameters determining the conditions of the plant leaf extract (such as types of phytochemicals, phytochemical concentration, metal salt concentration, pH, and temperature) are admitted to controlling the rate of nanoparticle formation as well as their yield and stability. The phytochemicals present in plant leaf extracts have a high potential to reduce metal ions in a much shorter time as compared to fungi and bacteria, which demands a longer incubation time. Therefore, plant leaf extracts are considered to be an excellent and benign source for metal as well as metal oxide nanoparticle synthesis. Additionally, plant leaf extract plays a dual role by acting as both reducing and stabilizing agents in the nanoparticles synthesis process to facilitate nanoparticle synthesis. The composition of the plant leaf extract is also an important factor in nanoparticle synthesis, for example, different plants comprise varying concentration levels of phytochemicals (Sorbiun *et al*., 2018).

The main phytochemicals present in plants are flavones, terpenoids, sugars, ketones, aldehydes, carboxylic acids, and amides, which are responsible for the bio-reduction of nanoparticles. Flavonoids contain various functional groups, which have an enhanced ability to reduce metal ions. The reactive hydrogen atom is released due to tautomeric transformations in flavonoids by which enol-form is converted into the keto-form. This process is realized by the reduction of metal ions into metal nanoparticles. In sweet basil (*Ocimum basilicum*) extracts, enol- to keto-transformation is the key factor in the synthesis of biogenic silver nanoparticles. Sugars such as glucose and fructose that exist in plant extracts can also be responsible for the formation of metallic nanoparticles. Note that glucose was capable of participating in the formation of metallic nanoparticles of different sizes and shapes, whereas fructose-mediated gold and silver nanoparticles are monodisperse (Kumar *et al*., 2013).

Synthesis of the nanoparticle by using Bacteria

Because of rapid development, affordable culturing costs and easy control and manipulation of the growth environment, bacteria are targets in the production of nanoparticles. At the same time, it is known that some species of bacteria have special mechanisms to suppress the toxicity of metals or heavy metals. Bacteria preferred for these properties can perform nanoparticle synthesis in-situ and ex-situ. Through the use of biochemical pathways and reducing agents such as proteins, enzymes, etc. which are present in the bacteria, metal ions can be reduced and precipitated for nanoparticle production (Greish *et al*., 2012).

Synthesis of the nanoparticle by using Fungi

NPs (5-50 nm) could be synthesized by extracellular using *Fusarium oxysporum*, with no evidence of flocculation of the particles even a month after the reaction. The long-term stability of the nanoparticle solution might be due to the stabilization of the silver particles by proteins. The 15 morphology of NPs was highly variable, with generally spherical and occasionally triangular shapes observed in the micrographs (Sylvestre *et al*., 2004).

Synthesis of the nanoparticle by using Algae

Algae are eukaryotic aquatic photosynthetic and they break down metallic salts into nanoparticles by their pigments, proteins, carbohydrates, fat, nucleic acid and secondary metabolites they contain. The algae extract that exists in an aqueous medium at a certain temperature is supplemented with metal solutions of the corresponding pH and concentration, and hence the synthesis of nanoparticles is achieved which may have antimicrobial properties without producing any toxic by-products during the synthesis. The size of nanoparticles is determined by certain parameters such as the incubation time of the solution, the ambient temperature, the pH of the mixture used and the metal ion concentration. Algae also provide an advantage to this synthesis method by their easy availability and usefulness. In addition, effective biomolecules in the reaction medium in the use of bacteria and plant extracts are less extinguished by the nanoparticles formed (Firdhouse *et al*., 2015).

2.7. Advantage of Bimetallic Nanoparticles over Monometallic Nanoparticles

In bimetallic nanoparticles, two different metals combine to show novel properties which are the combination of the two metals present in it. This makes them more important than of MMNPs for industrial as well as for the technological point of view. Bimetallic nanoparticles are more important as compared to those of monometallic nanoparticles due to the presence of an extra degree of freedom. The catalytic properties of gold can be enhanced to a greater extent by mixing it with some other metals such as silver or nickel or cobalt, etc. BMNPs have a greater surface area which increases their adsorption power and hence acts as efficient catalysts as compared to those of monometallic nanoparticles (Khatami *et al*., 2018).

2.8. Unique Properties of Bimetallic Nanomaterial

Properties of BMNPs are influenced by both the metals; they provide excessive ordinary metallic NPs, which is an advantage. The properties of alloy NPs can be extremely different from those of the elemental monometallic nanoparticles (Srinoi *et al*., 2018a).

Optical properties of BMNPs: Plasmonic coupling between NPs is one of the most interesting optical properties; the characteristic improvement of the local optical field at the particle-particle interface is extremely useful for numerous sensing applications. Monometallic NPs have relatively monotonous optical properties due to surface plasmon resonance (SPR); the SPR properties of alloy BMNPs are incessantly tunable because of the possibility of composition changes. SPR excitation within the nanostructures greatly enhances the local electric field. The absorption and dispersion of light in NPs rely on the characteristic of the metals, including their chemical composition, morphology, and size. NPs of noble metals, for instance, gold and silver, with a size smaller than the wavelength of visible light powerfully scatter and absorb light because of SPR. Au/Ag BMNPs show diverse optical responses for alloy and core-shell configurations, even when they have the same Au and Ag contents (Tiwari *et al*., 2020).

Antibacterial properties: BMNPs show high-quality antibacterial activity against Gram-positive bacteria and Gram-negative bacteria (Kumar *et al.*, 2013). Ag-Mn nanoparticles were synthesized by co-reduction of $AgNO_3$ and $KMnO_4$ solution using *A. pintoi* extract as a combined reducing and stabilizing agent. The Physico-chemical properties of the obtained Ag-Mn NPs were investigated. The antibacterial feature of silver-manganese nanoparticles was evaluated throughout against gam (−) bacteria including *Escherichia coli (E. coli), Salmonella typhimurium* (*Salmonella),* and *Pseudomanas aeruginosa (P. aeruginosa)*; and gram (+) bacteria: *Staphylococcus aureus (S. aureus)* and *Bacillus cereus (B. cereus* (Arora *et al*., 2020).

The antibacterial effectiveness of silver and silver/gold BMNPs against the anaerobic oral pathogen is observed. Since oxidative stress is one of the main causes of the inflammatory environment found in the periodontal pocket, its physiological level has been simulated by the addition of hydrogen peroxide *in vitro*. So in this study, we also determined the effects of (0.1–0.25mM) hydrogen peroxide-induced stress on the antibacterial activity of Ag and Ag/Au NPs against the anaerobic oral pathogen (Al *et al*., 2020).

Catalytic properties: A novel group of materials for catalysis have been densely studied, that is, “bimetallic nanoparticles”. Metal NP catalysts comprising two (or more) different metal components have received attention from both technological and scientific points of view for improving the quality or properties of catalysts (Dietrich *et al*., 2021).

2.9. Garlic Plants (*Allium Sativum L*)

Garlic (*Allium sativum L.)* is one of the most important Allium plants widely cultivated throughout the world including Ethiopia for use as a spice, food flavoring agent and medicinal value. Garlic (*Allium sativum*) is a species in the onion genus, *Allium.* Its close relatives include the onion, shallot, leek, chive, and Chinese onion It is native to Central Asia and northeastern Iran and has long been a common seasoning worldwide, with a history of several thousand years of human consumption and use It was known to ancient Egyptians and has been used as both a food flavoring and a traditional medicine China produces some 80% of the world's supply of garlic (Kasim *et al*., 2019).

Garlic is easy to grow and can be grown year-round in mild climates. While sexual propagation of garlic is possible, nearly all of the garlic in cultivation is propagated asexually, by planting individual cloves in the ground. In colder climates, cloves are best planted about six weeks before the soil freezes. The goal is to have the bulbs produce only roots and no shoots above the ground. Harvest is in late spring or early summer. Garlic plants can be grown closely together, leaving enough space for the bulbs to mature, and are easily grown in containers of sufficient depth. Garlic does well in loose, dry, well-drained soils in sunny locations, and is hardy throughout. Garlic plants prefer to grow in soil with a high organic material content but are capable of growing in a wide range of soil conditions and pH levels (Tyagi *et al*., 2013).

There are different varieties or subspecies of garlic, most notably hard neck garlic and soft neck garlic. The latitude where the garlic is grown affects the choice of type, as garlic can be day-length sensitive. Hard neck garlic is generally grown in cooler climates and produces relatively large cloves, whereas soft neck garlic is generally grown closer to the equator and produces small, tightly-packed cloves. Garlic scapes are removed to focus all the garlic's energy into bulb growth. The scapes can be eaten raw or cooked (Ayalew *et al*., 2015).

Figure 2.7: garlic plant (Ayalew *et al*., 2015).

2.10. Characterization Techniques of Bimetallic Nanoparticles

Identifying and studying the physicochemical properties, structure details, purities, and dopants of biosynthesized NPs is very important as the structure, size, shape of NPs can significantly affect their performance and properties. Determining the physicochemical characteristics of NPs helps to effectively understand the relationship between these characteristics and their performance. Describing the behavior and structure of green synthesized NPs is quite difficult due to the existence of various macromolecules in their extract which participate in their structure (Khatami *et al.*, 2018). Common physicochemical characterization techniques of BMNPs are:

2.10.1. X-ray diffraction methods

The powder XRD is the most common and first-hand instrument used by solid-state scientists. X-ray diffraction is a powerful method to investigate the detailed structure, composition and related properties of nano-materials. This information can be derived from peak position, intensity and the peak profile. A great advantage of X-ray powder diffraction is that it requires virtually no sample preparation, in comparison to other techniques. The sample can be either in the form of a smear or compact flat pack or a capillary and is exposed to a monochromatic beam of X-ray and the diffracted beam intensity is collected in a range of angles (2θ) to the incident beam. The intensity corresponding to constructive interference of the diffracted beam from a crystallographic plane is observed as peak, corresponding to the Bragg angle (θ). In all other angles, a background is obtained. The intensity corresponding to the background has several origins. During the analysis of XRD measurement, X-Rays were directed towards the sample specimen and proceed to elastically scatter the electron clouds of atoms in the sample. The detector was then used to measure the X-Ray intensity as a function of the angle of beam diffraction. A periodic structure within the sample leads to interference fringes determined by the periodic arrangement of the atoms (Cullit and Stock, 2001).

For core-shell, alloys and hetero-structure of bimetallic nanoparticles the XRD on a laboratory instrument is able to distinguish between physical mixtures of both metals and bimetallic nanoparticles phases. It also possible to separate the core from the shell in the bimetallic core-shell bimetallic nanoparticles due to the different domain size and because it was known which metal is the core and which metal is the shell. Thus Bragg's Law Eqn. (2.1) plays a crucial role in the interpretation of these peaks.

$$\lambda = 2d\sin\theta \qquad (2.1)$$

Where, d - the distance between the atomic planes

θ Being the diffraction angle and

λ - The wavelength of the incident X-ray radiation

In addition to determining the crystal phase, the line widths can be used to estimate the mean crystal size of a sample by use of Scherrer's equation (2.2) (Rostek *et al.*, 2019).

$$D = K\lambda / \beta \cos\theta \tag{2.2}$$

Where, D is the mean size of the crystalline domains, which may be smaller or equal to the grain size, K is a dimensionless shape factor with a value close to unity, λ is the X-ray wavelength, which depends on the X-ray sources used, β is the line broadening full width at half maximum intensity (FWHM) in radians and θ is the Bragg's angle of diffraction.

The dislocation densities of synthesized NPs are calculated from:

$$\delta = \frac{1}{D^2} \tag{2.3}$$

Where δ is the dislocation density, D is the crystalline size.

The micro-strain is estimated from Equation (2.4) below:

$$\varepsilon = \frac{\beta}{4\tan\theta} \tag{2.4}$$

The value of lattice parameter is calculated as: for hexagonal crystal structure

$$\frac{1}{d^2hkl} = \frac{4}{3a^2} \times (h^2 + hk + k^2) + \frac{l^2}{c^2} \tag{2.5}$$

Where d is d-spacing, (h,k,l) were miller indices and (a, c) are lattice parameter

2.10.2. Ultraviolet-Visible Spectroscopy (UV-Vis)

(UV-Vis) refers to absorption spectroscopy or reflectance spectroscopy in the ultraviolet-visible region. The UV-visible range is only a small part of the total electromagnetic spectrum and is generally defined from wavelengths of 190 nm at the high energy UV end to about 750 nm at the low energy red end of the spectrum. Light of other regions of the spectrum gives rise to different types of transitions and hence different types of spectroscopy (Atomssa & Gholap, 2011).

The energy band gap for the samples are calculated from the Tauc relations (Jubu *et al*., 2020).

$$(\alpha h v)^2 = \kappa(hv - E_g) \tag{2.6}$$

Where α = absorbance co-efficient, h = Plank constant, v = Frequency of incident Uv-radiation, k = Constant, hv = Energy, E_g = Band gap energy

$$E_g = \frac{1240}{\lambda_{\max}} \text{ (eV)} \tag{2.7}$$

Absorbance co-efficient (α) is calculated as

$$\alpha = 2.303 \times \frac{A}{t} \tag{2.8}$$

Where A = absorbance and t is the thickness of the cuvette. Thus its value is 1 cm.

Absorption coefficient measures the light that might be absorbed by a given thickness of the sample; it tells us how much light corresponding to a specific wavelength will be absorbed by materials (Jubu e*t al*., 2020)

2.10.3. Scanning Electron Microscope (SEM)

Scanning electron microscopy (SEM) is a technique in which a highly focused beam of high-energy electrons interacts with a sample to produce various signals that contain information about the topography, morphology and crystallography of the sample. Most data is collected over a selected area of the surface of the sample, and a 2-D image that displays spatial variations in these properties is generated. In a typical SEM system, a beam of accelerated electrons with significant amounts of kinetic energy strikes the surface of the sample and generates a splash of electrons with kinetic energies much lower than primary incident electrons called secondary electrons (that produce SEM images). To create an SEM image, the secondary electron intensity was measured as a function of the primary beam position (Esparza *et al*., 2015).

2.10.4. Fourier transform infrared spectroscopy (FTIR)

In FTIR spectroscopy we look at the changes in the vibrational motion of atoms in a molecule, which are greatly influenced by the masses of atoms, their geometrical arrangement and the strength of their chemical bonds. FTIR involves IR radiation and results from the transition between quantized vibrational states and provides a complimentary image of molecular vibrations. Thus the interaction of IR radiation with the vibrating molecule is only possible if the molecular dipole moment is modulated by the vibration (IR active). IR encompasses a spectral region from the red end of the visible spectrum ($12500cm^{-1}$ to the microwave ($10cm^{-1}$) the region in the electromagnetic spectrum. This infrared region is divided into near IR ($12500\ to\ 4000\ cm^{-1}$, mid-IR ($4000\ to\ 400\ cm^{-1}$) and far IR ($400\ to\ 10\ cm^{-1}$). FTIR spectrometers are based upon the Michelson interferometer (Hjältén *et al*., 2021).

2.11. Application of Bimetallic Nanoparticles

Bimetallic nanoparticles hold numerous applications including electrical, optical, catalytic and biomedical. BMNPs serve as very good catalysts. The use of BMNPs makes it possible not only to obtain better catalytic activity but also helps in making new materials having desired properties that cannot be achieved by a single metal atom. Bimetallic nanoparticles unveil interesting electronic, chemical, biological, mechanical and thermal properties due to their composition and synergistic effects. The activity, as well as the selectivity of the catalyst, is affected by the size of the particle. The use of bimetallic nanoparticles may give rise to synergism when the particles are used for catalysis. The combination of two different metals enhances their specific properties. These properties may be different from those of pure elemental particles. The elemental arrangement of bimetallic nanoparticles depends strongly on the method used for their production and the system of two metals is generally not in thermodynamic equilibrium (Khatami *et al*., 2018).

Core-shell bimetallic particles are among the most studied Nano-catalysts. Metallic and bimetallic nanoparticles, especially those containing a few tens or few hundreds of atoms, are excellent catalysts because of their highly active surfaces. These catalytic nanoparticles have improved selectivity, efficiency and recyclability, achieving the modern requirement for green catalysts. In the preparation of bimetallic nanoparticles, the interaction between two metals plays an important role. In pharmaceutical sciences, these are used to reduce the toxicity and side effects of the drugs. Nanoparticles can also be used in our everyday life. For instance, BMNPs are used in many popular sunscreens. Nanotechnology is a refractive index for various surfaces and also provides light-based sensors for use in diagnosing cancer. Underlying are some major application fields of bimetallic nanoparticles and nanocomposites (Mazhar *et al*., 2017).

2.11.1. Anti-bacterial Application of Bimetallic Nanoparticles

Highly effective antimicrobial agents are needed to control the emergence of new bacterial strains, their increased growth capability, and antibacterial resistance that severely impact public health, and several industries including water, food, textiles, and oil and gas. Recently, BMNPs, formed via the integration of two different metals, have appeared particularly promising with antibacterial efficiencies surpassing that of monometallic counterparts due to synergistic effects, the broad range of physiochemical properties, and diverse mechanisms of action (Huynh *et al*., 2020).

In general, the antimicrobial activity of BMNPs has been evaluated against various types of pathogenic bacteria, indicatively being tested against *Staphylococcus aureus*, *Escherichia coli*, *Streptococcus mutans*, and *Pseudomonas aeruginosa*, which are mainly accountable for many human epidemics (Arora *et al*., 2020). These NPs typically exhibit superior performance compared to conventional antibiotics and antimicrobial treatments since microorganisms cannot generate resistance to them since the BMNPs suppress the formation of biofilm and activation of other associated processes, thus outwitting the mechanism of drug resistance. Notably, unlike conventional antibacterial agents, these nanomaterials can also be employed to carry and deliver additional antibacterial drugs, i.e., operate as drug delivery scaffolds, while they can also exhibit antimicrobial activity by themselves (Jong & Paul, 2008). Interestingly, the side toxicity of various metal-based NPs has been observed to be relatively neutral toward the environment and humans when the NP dosage is provided at an optimal level sufficient to only suppress the microbial growth (Basavegowda *et al*., 2020).

2.11.2. Biomedical

Special nanoparticles have been prepared that helps in the early diagnosis of disease in the human body. These can also be used for the determination of nutrient levels in the body. Magnetic bimetallic nanoparticles or nanoparticles have been used for the controlled drug delivery. Controlled drug delivery systems have some specific goals such as maintaining biocompatibility during the action, therapeutic processes and faster production. The release rate of these drugs depends upon the diffusion coefficient and biodegradation rate. Bimetallic nanoparticle offers an alternative to the traditionally used drug delivery system due to their high specificity. Magnetic bimetallic nanoparticles when injected inside the body reach their target site under the influence of an external magnetic field and helps in eliminating infected cells. Conjugation of specific proteins such as antibodies to the bimetallic nanoparticle surface has been abundant potential for greater specificity and immunologically directed targeting (Venkatesh *et al*., 2018).

2.11.3. Magnetic

Nanoparticles have the potential of increasing the density of various storage media devices and when magnetized they can improve the detail and contrast of magnetic resonance imaging (MRI) images. These nanoparticles are coated with a peptide that specifically binds to the tumor cells. After their attachment, the bimetallic nanoparticles help in improving the MRI imaging. These are also used in capacitors for storing energy. Magnetic bimetallic nanoparticle-containing iron oxide allows the nanoparticles to be directed towards the stents by the magnetic field. This allows the specific delivery of these drugs to the stents placed in arteries (Srinoi *et al*., 2018b).

3. MATERIALS AND METHODS

In this chapter, the study site, materials and methods of the experiment were presented. The first part of the chapter covered the study site, various chemicals, samples and instruments required to carry out this research and in the second section of this chapter, synthesis methods of different samples for bimetallic synthesis, characterization methods and how to check the application of Ag NPs and Ag/Zn BMNPs against selected bacterial species were presented.

3.1. Study Sites Description

Green Synthesis of Ag/Zn BMNPs using *Allium sativum L* plant Extract, characterizations and its application for anti-bacterial were carried out in Applied Chemistry Department Laboratory which located in Adama Science and Technology University. Uv-vis spectroscopy and Scanning Electron Microscopy (SEM) characterization of the synthesized nanoparticles were performed in the Applied Biology Department laboratory in ASTU, XRD spectroscopy characterization was carried out in the Materials Science engineering Laboratory and FTIR analysis was also performed in Addis Ababa University. The anti-bacterial activity study of the nanoparticles was also worked in the Applied Biology Department laboratory in the School of Applied Natural Science.

3.2. Materials

The following were among the various chemicals, samples, and laboratory apparatus used for this Thesis research work.

3.2.1. Chemical and Samples

The chemicals and reagents required for the preparation of Ag NPs and Ag/Zn BMNPs were distilled water, zinc nitrate hexahydrate ($Zn(NO_3)_2.6H_2O$, silver nitrate ($AgNO_3$), ethanol, Agar and garlic (*Allium sativum L*) plant. Gram-positive and Gram-negative bacterial strains were required. All the chemicals were analytical grade. Those reagents were brought commercially from chemical stores in Addis Ababa and garlic plant was also purchased from Adama local market.

3.2.2. Apparatus and Instrumentations

3.2.2.1. Apparatus

The following laboratory apparatus and instruments were used for the experiments: beaker, measuring cylinder, pipettes, volumetric flasks, magnetic stirrer with hot plate, funnel, filter paper, quartz cuvettes, analytical balance, dropper, centrifuge, petri-dish and crucible.

3.2.2.2. Instruments

The laboratory instruments that were used for characterizing the synthesized NPs were mentioned as follows: UV-Vis spectroscopy was used to study the optical properties of the nanoparticles, SEM was used to study the composition, texture, and morphology of the prepared nanoparticle, FITR was used to characterize the vibrational motions of atoms in the molecules, XRD was used to characterize the nature of crystal structure of the synthesized Ag NPs and Ag/Zn BMNPs.

3.3. Methods

3.3.1. Preparation of the Garlic Plant Extract

The preparation of garlic plant extract was carried out using a modified procedure reported by Gupta *et al*., (Gupta, *et al*., 2020). Garlic (*Allium sativum L*.) plant was collected from Adama local market. Then, the plant was washed several times with tap water and with distilled water to remove the dust particles and then its skin was peeled off and dried in light at room temperature. The cleaned dried plant was cut and ground to make powder before using it for the synthesis of NPs. 100 g of garlic (*Allium sativum L*) plant powder was added into 1000 mL conical flask and 600 mL of distilled water was also added to the flask; then the mixtures were heated at 40 ℃ for 30 min. After 30 min, the heater was turned off and the mixtures were stirred for 1 hr as shown in Figure 3.1. After a while, the mixture was allowed to settle. Then after settlement, the extract was filtered with Wattman No 1 filter paper to get a clear solution for further experiments (Gupta, *et al*., 2020).

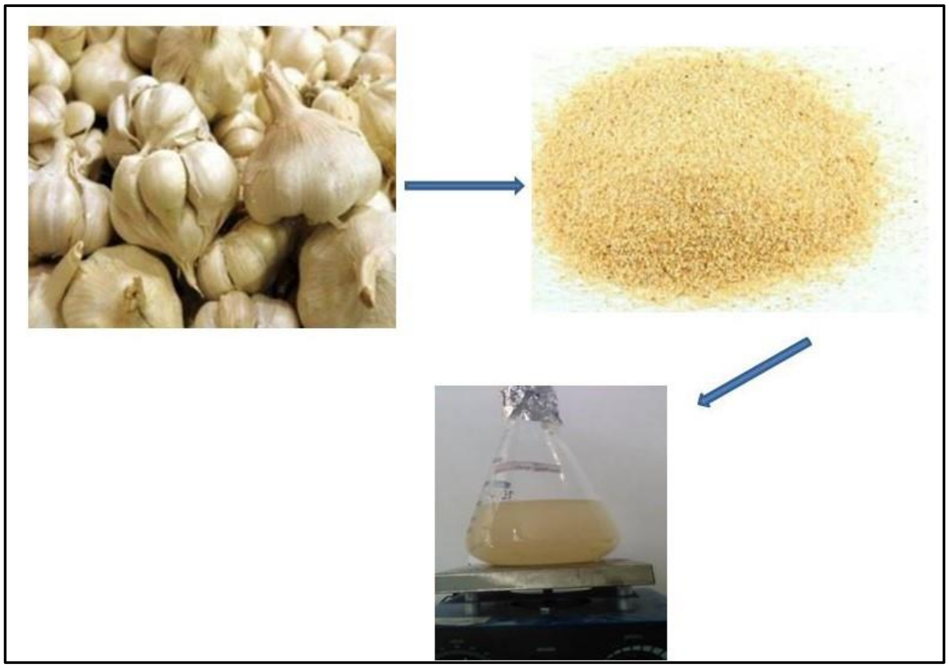

Figure 3.1: Preparation of the extract of garlic plant.

3.3.2. Phytochemical Qualitative Analysis of Aqueous Extract of Garlic (*Allium sativum L*)

The plant extract was subjected to assessment for the existence of the phytochemicals by using the following standard methods (Gul *et al*., 2017), (Lemilemu *et al*., 2020).

1. **Tests for Flavonoids (Alkaline Reagent Test)**: 2 mL of 2.0% NaOH mixture was mixed with aqueous plant crude extract; concentrated yellow color was produced, which became colorless when 2 drops of diluted acid were added to the mixture. This result showed the presence of flavonoids.
2. **Alkaloids (Wagner's test)**: 2 mL of aqueous plant extract solution was dissolved in Wagner's reagent (Iodine in Potassium Iodide). The formation of brown/reddish precipitate was shown the presence of Alkaloids.
3. **Test for tannins**: 0.5 g of plant extract was boiled in 10 mL of distilled water in a test tube and filtered. 5 drops of 0.1 % $FeCl_3$ were added to the filtrate, to give a brownish-green or a blue-black color which confirms the presence of tannins.
4. **Test for terpenoids (Salkowski test)**: 2 mL of aqueous plant extract was mixed with 2 mL of chloroform and 3 mL concentrated H_2SO_4 carefully to form a layer. A

reddish-brown coloration of the interface was formed to show positive results for the presence of terpenoids.

5. **Test for Steroids**: 2 mL of chloroform and concentrated H_2SO_4 were added with the 5mL aqueous plant crude extract. In the lower chloroform layer, the red color appeared that indicated the presence of steroids.
6. **Tests for Glycosides (Salkowski's Test)**: We added 2 mL H_2SO_4 concentrated to the aqueous plant crude extract. A reddish-brown color formed which indicated the presence of steroidal aglycone part of the glycosides.
7. **Test for phytosterols (Salkowski's test)**: 2 mL of aqueous plant extract and 10 mL of chloroform were added and then filtered. 5 drops of concentrated H_2SO_4 were added to the filtrate; the mixture was shaken and examined for the appearance of the golden yellow color.
8. **Test for Anthraquinones**: 10 mL of benzene was added in 6 g of the garlic plant powder sample in a conical flask and soaked for 10 minutes and then filtered. Further 10 ml of 10% ammonia solution was added to the filtrate and shaken vigorously for 30 seconds and pink, violet, or red color indicated the presence of anthraquinones in the ammonia phase.
9. **Test for saponins**: 0.5 g of plant extract was taken then 5 mL of distilled water was added and shaken while heating to boil. Frothing showed the presence of saponins.
10. **Test for phenols**: 5 drops of 2 % of $FeCl_3$ were added to 2 mL of aqueous plant extract and the formation of bluish-green to black color indicates the presence of phenols.

3.3.3. Preparation of 0.1 M of $AgNO_3$ Solution and 0.1 M $ZnNO_3$ Solution

500 mL of 0.1 M $Zn(NO_3)_2$ solution was prepared by taking 14.875 g of $Zn(NO_3)_2$ salt and added into 500 mL of round bottom flask then distilled water was added and shaken to get a homogenous mixture. Finally, the distilled water was filled into the round bottom flask until its mark (Patra *et al*., 2017).

500 mL of 0.1 M $AgNO_3$ Solution was prepared by taking 8.494 *g* of $AgNO_3$ salt and added into 500 mL of round bottom flask then distilled water was added and shaken to

get homogenous the mixture. Finally, the distilled water was filled into the round bottom flask until its mark (Patra *et al*., 2017).

3.3.4. Green Synthesis of Silver NPs

The green synthesis of Ag NPs has been carried out by adapting the reported procedure by Alahmad *et al.,* with minor modifications. The Ag NPs were prepared by taking 500 mL of 0.1 M $AgNO_3$ solutions and 100 mL of garlic plant extract in 1000 mL of beaker then the mixture was heated at 40 ℃ for 60 minutes on the hot plate with stirring. After cooling the liquid above was decanted and centrifuged for 30 min. finally, the solid part was washed with distilled water and ethanol then dried on a ceramic crucible for 5 days at room temperature. As depicted in Figure 3.2, finally, the powder of Ag NPs was obtained (Alahmad *et al*., 2021).

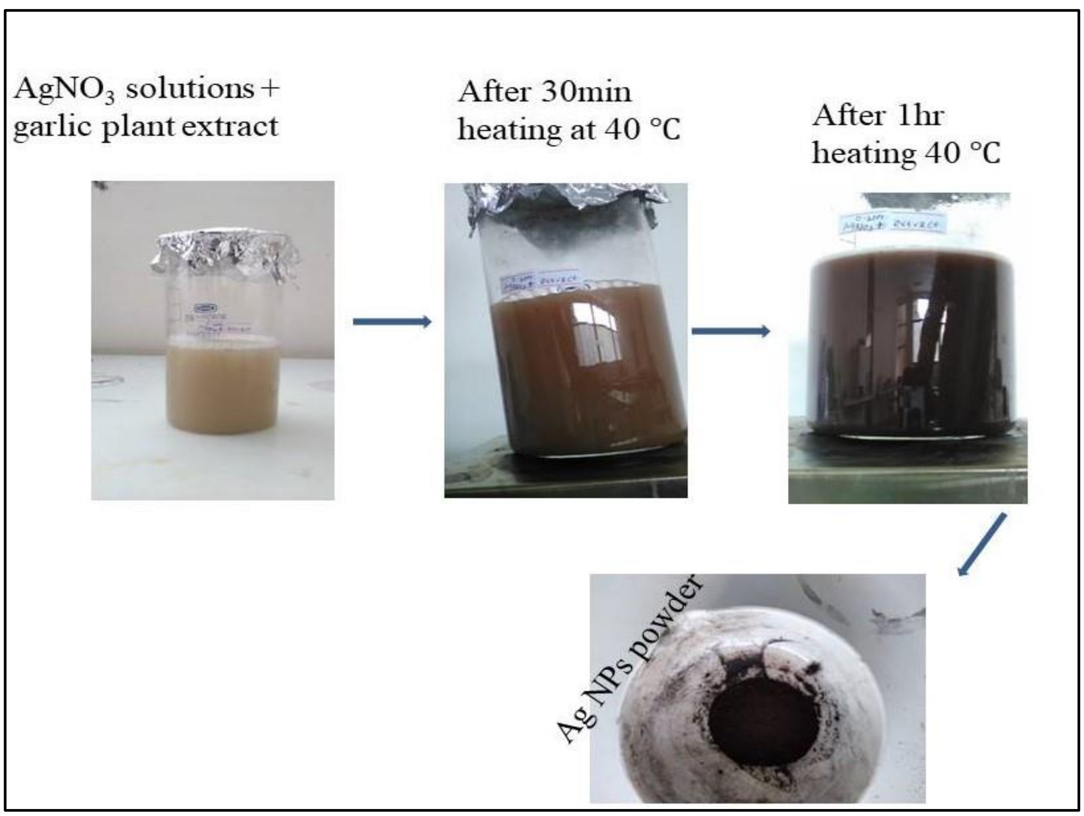

Figure 3.2: silver nanoparticle synthesis

3.3.5. Green Synthesis of Ag/Zn BMNPs

The green synthesis of Ag/Zn BMNPs has been carried out by using 0.1 M $AgNO_3$, 0.1M $ZnNO_3$ solution and garlic plant extract (Figure 3.3). 300 mL of 0.1 M $Zn(NO_3)_2$ solution was added to the 1000 mL beaker then it was heated at 40 ℃ for 15 min; then 300 mL of 0.1 M $AgNO_3$ solution was added to the beaker while heating and stirring for 15 min again. After 15 min the heater was removed. Then 100 mL of plant extract was added to the solution from the buret a drop-wise with the constant stirring for 1hr; then the mixture was kept for the formation of the precipitate. After a while, the precipitated mixture was centrifuged for 30 min. Finally, the solid part was washed with distilled water and ethanol then dried on a ceramic crucible for 5 days at room temperature. Finally, the black powder of Ag/Zn BMNPs was be obtained (Nadeem *et al*., 2019).

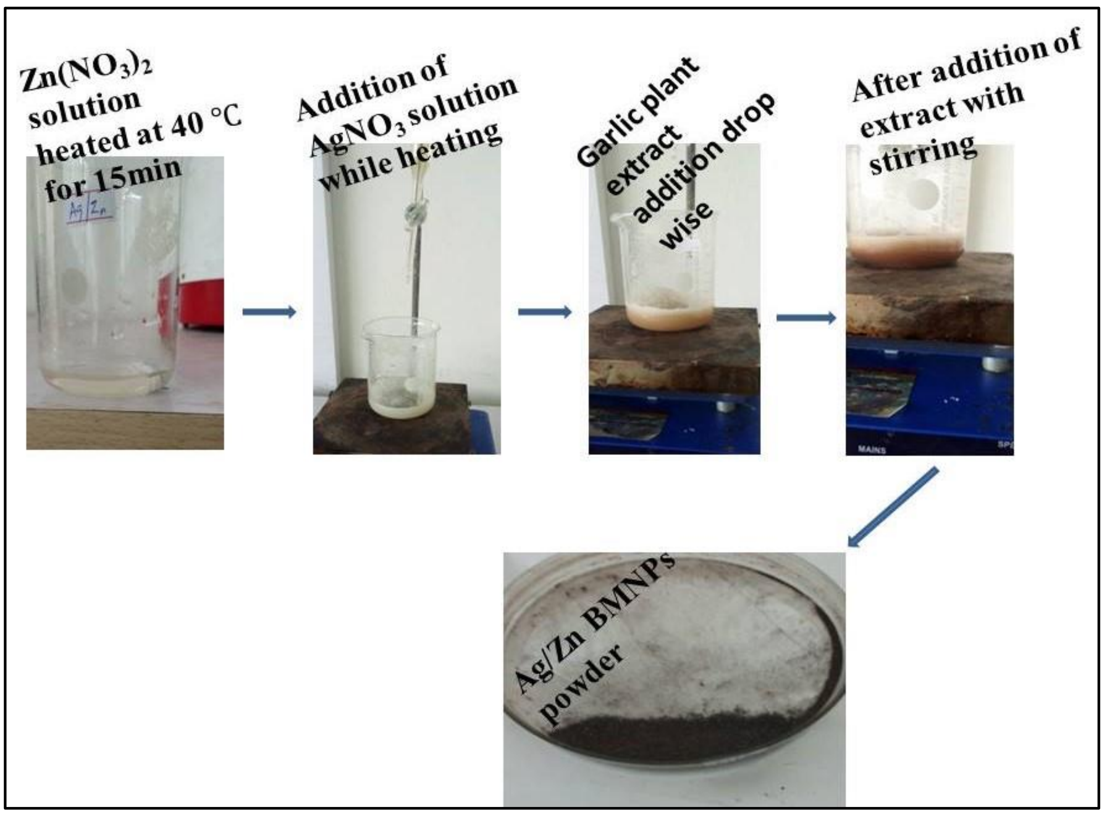

Figure 3.3: Preparation of Ag/Zn BMNPs.

3.4. Characterization Techniques of Ag NPs and Ag/Zn BMNPs

The UV-Vis absorption peaks of synthesized nanoparticles were recorded in the range of 200–800 nm with UV-Vis spectroscopy (PerkinElmer, Lambda 19 Spectrophotometer).

The ASCII files of the measured spectra were collected by the computer which interfaced with the instrument. FT-IR spectra were recorded using KBr pellets (Perkin Elmer) in the range of 400–4000 cm^{-1}. The powder sample is mixed with nujol oil to form a thick pellet and held between salt plates or thoroughly mixed with potassium bromide (KBr) and pressed using a hydraulic press to form pellets and then placed in the sample holder of the instrument. XRD technique was used to reveal the crystalline nature of synthesized Ag NPs and Ag/Zn BMNPs. XRD is equipped with Cu-Kα radiation (λ=0.154056 nm) and operates at a voltage of 40 kV and applied current of 30 mA in the scanning speed of 3.00 degrees per minutes which in turn the collected data were scanned in the range of 2θ=10° $\leq 2\theta \leq 80°$. SEM was used for understanding morphological and structural features of synthesized NPs using (JEOL, JCM-6000Plus). SEM characterization, NPs powder was mounted on a sample holder followed by coating with a conductive metal. The samples were then scanned with a focused fine beam of electrons. (Murthy *et al*., 2020).

3.5. Evaluation of the Antibacterial Activity and Application of Ag NPs and Ag/Zn BMNPs

The antibacterial activity of the NPs on gram-negative species *E. coli* and *P. aeruginosa* and gram-positive species, *S. pyogenes* and *S. aureus* were tested by the disc diffusion agar method. Bacterial species were grown aerobically in the presence of oxygen in nutrient broth for 24 hrs at 37 ℃ before using as a target organism. The Ag NPs and Ag/Zn BMNPs synthesized from garlic plant extracted solutions of 20 mL were dispersed in 50 mL of DMSO and stirred using a magnetic stirrer for 30 min. From this solution about different concentrations (100μg/ml, 50μg/ml, 25μg/ml and 12.5μg/ml) were poured using a micro pipette in each pathogen well. After inoculation and cultivation of apply target bacterial on top of Mueller Hinton agar. Finally, the diameters of the inhibition zones were measured in millimeters after 24 hrs incubation times (Karnib *et al*., 2013).

4. RESULTS AND DISCUSSION

In the first section of this chapter, the results of the phytochemical screening of *Allium sativum L* plant extract were presented. In the second section, crystal size, lattice parameters, micro-strains and dislocation densities of Ag NPs and Ag/Zn BMNPs by X-ray diffraction were presented. In the third section, the UV-Vis absorption spectra and calculated band gaps of those synthesized NPs were presented. In the fourth section of this chapter, the SEM analysis was discussed. In the fifth section, the functional groups and their assignments of synthesized NPs were presented briefly. In the last section, the antibacterial activities of synthesized were discussed.

4.1. The Phytochemical screening test results

The preparation of the garlic (*Allium sativum L.*) extract by aqueous extraction of the dried and ground plant was the initial activity carried out for the green synthesis of the metallic and bimetallic nanoparticle. Then to understand the phytochemicals responsible for the reduction and/or capping of the nanoparticle synthesized, the phytochemical screening of the extracted garlic (*Allium sativum L.*) has been carried out. Accordingly, the results of the phytochemical analysis for the extract of garlic (*Allium sativum L.*) are summarized in Table 4.1 below. The data obtained revealed that the garlic (*Allium sativum L.*) is primarily composed of flavonoids, tannins, terpenoids, glycosides, phytosterols, saponins and phenols which are responsible for the facilitation of the synthesis of both Ag NPs and Ag/Zn BMNPs. As reports by Ovais *et al.*, indicates the Phyto-components of plant extracts act as reducing as well as stabilizing agents. (Ovais *et al.*, 2018). The flavonoids can be used as reducing agents for the preparation of biocompatible NPs because they belong to substances with relatively low affinity to the metal surface (they do not contain in their structures sulfur or nitrogen atom), which means adsorption of analyte molecules can be quite simple as the report by Švecová *et al.*, showed (Švecová *et al.*, 2018). The role of terpenoids and polyols of the plant extract in the reduction and stabilization of nanoparticles was confirmed on an infrared spectrum. Subsequently, the crystal structure transformed from monoclinic to a cubic system and increased in size the report by Kumar *et al.*, (Kumar *et al.*, 2019).

Table 4.1: Results of Phytochemical Screening of *Allium sativum L* plant

s.no	Secondary Metabolite	Results
1	Flavonoid	+
2	Alkaloid	-
3	Tannins	+
4	Terpenoid	+
5	Steroid	-
6	Glycosides	+
7	Phytosterols	+
8	Anthraquonins	-
9	Saponins	+
10	Phenol	+

4.2. X-ray diffraction (XRD) analysis

The XRD patterns of Ag NPs and Ag/Zn BMNPs were shown in Figure 4.1. For Ag NPs diffraction peaks were observed at 2θ values, 38.38°, 44.23°, 64.60° and 77.58° which corresponds to (111), (200), (220) and (311) plane respectively. The spectral data revealed that the synthesized Ag NPs showed cubic phase and the observed peaks were fitted with the Joint Committee on Powder Diffraction Standard (JCPDS card No. 004-0783, space group Fm-3m). In addition, the XRD pattern of synthesized Ag NPs depicts that, sharp and intense peaks, revealing that the prepared samples were of good crystalline nature. As the report by Jha & Prasad Ag NPs showed the space group Fm-3m (Jha & Prasad, 2010) which confirms the synthesized Ag NPs in this research work.

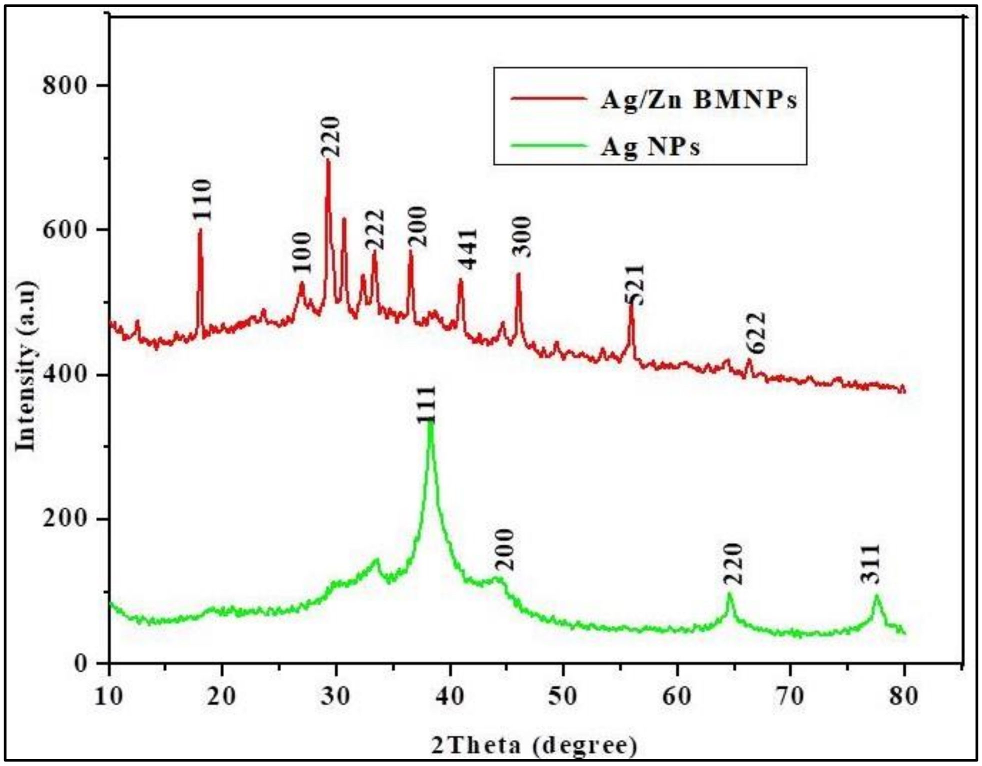

Figure 4.1: X-ray diffraction patterns Ag NPs and Ag/Zn BMNPs

The XRD patterns of Ag/Zn BMNPs shows peaks at 2θ = 18.04°, 26.92 °, 29.36°, 33.38°, 36.59 °, 40.95°, 46.04 °, 55.91° and 66.44 ° which are indexed to (110), (100), (220), (222), (200), (441), (300), (521) and (622) respectively. From those peaks the peaks indexed at (220), (222), (441), (521) and (622) indicates the Ag/Zn BMNPs phases. While the peaks indexed at (110) and (100) shows the ZnO NPs phase, the (200) peak Ag NPs and the (300) peak depicted the Ag_2O NPs. The spectral data obtained depicted that the synthesized Ag/Zn BMNPs showed cubic crystal structure phase and the observed peaks were fitted with the Joint Committee on Powder Diffraction Standard (JCPDS card No. 026-0956, space group I-43m). The sharp and intense peaks observed in the XRD spectra of synthesized Ag/Zn BMNPs indicated that the Ag/Zn BMNPS synthesized were of good crystalline nature. The average crystallite size of the prepared nanoparticles is estimated by using Scherrer's formula (equation 2.2) (Vorokh, 2018).

For the synthesized Ag NPs and Ag/Zn BMNPs the d-spacing (d), particle size (D), dislocation density (δ) and microstrain (ε) were calculated using equation (2.1- 2.4) and presented in the table (4.2-4.3) below for the strongest peaks of respective synthesized NPs.

Table 4.2: The calculated parameters for the strongest peaks of Ag NPs

2θ (deg)	θ(deg)	FWHM (β) (deg)	β(rad)	d ($A°$)	D (nm)	$\delta \times 10^{-3} (nm^{-2})$	$\varepsilon \times 10^{-3}$
38.38	19.19	1.34	0.023	2.34	6.30	25.20	16.75
44.23	22.11	1.52	0.026	2.04	5.64	31.44	16.31
64.60	32.30	0.77	0.013	1.44	12.20	6.72	5.32
77.54	38.77	0.78	0.013	1.23	13.11	5.81	4.23

The average crystallite size of the Ag NPs calculated is 9.31 nm

Similarly, for Ag/Zn BMNPs the d-spacing (d), particle size (D), dislocation density (δ) and microstrain (ε) were calculated and tabulated in Table 4.3.

Table 4.3: The calculated parameters for the strongest peaks of Ag/Zn NPs

2θ (deg)	θ(deg)	FWHM (β) (deg)	β(rad)	d ($A°$)	D (nm)	$\delta \times 10^{-3}$ (nm^{-2})	$\varepsilon \times 10^{-3}$
29.36	14.68	0.54	0.0093	3.04	15.36	4.24	8.91
33.38	16.69	0.48	0.0084	2.68	17.19	3.39	7.04
40.95	20.47	0.47	0.0083	2.20	17.87	3.13	5.55
55.91	27.95	0.46	0.0081	1.64	19.47	2.64	3.80

The average crystallite size of the Ag/ Zn BMNPs was deduced to be 17.47 nm.

The lattice parameter for the synthesized nanoparticles is calculated by the equation (2.5). Since the synthesized Ag NPs cubic in structure and Ag/Zn BMNPs phase are cubic in structure and there are also hexagonal structures for ZnO NPs phase observed in bimetallic structure. Since the intention is about Ag/Zn BMNPs the lattice parameters was calculated for cubic structures only. For cubic phase structure the lattice parameter is (a = c) are equal. Thus only the value of (a) was calculated and presented in tables (4.4).

Table 4.4: The calculated lattice parameter for Ag NPs and Ag/Zn BMNPs

Sample	2θ (deg)	Miller indices			d($A°$)	a=c ($A°$)
		h	k	l		
Ag NPs	64.60	2	2	0	1.44	5.76
Ag/Zn BMNPs	29.36	2	2	0	3.04	9.86

From the all calculated data above one can correlate the peak position (2θ), the average crystalline size (D) and microstrain (ε) and dislocation density as follows:
The decrease in the microstrain (ε) shows that the angle (2θ) or peak position increased, the average crystalline size is increasing as the peak position increases and this shows that the crystalline size is also contributing to peak broadening. Dislocation density measures the number of dislocations in a unit volume of crystalline materials. Thus, as the particle size of nanoparticles increases the dislocation density of the crystalline materials is decreased. In another word, as the peak position (angle) increases the dislocation density of the crystalline particle is decreases.

When the synthesized nanoparticles were compared, the synthesized Ag NPs and Ag/Zn BMNPs an average crystalline size of 9.31 nm and 17.47 nm respectively and peak position (2θ) are increased in these sequences. Since dislocation density depends upon particle size that means as particle size increases dislocation density decreases. Thus, the dislocation density decreases in the order of Ag NPs and Ag/Zn BMNPs

4.3. Uv- vis spectroscopy analysis

The optical properties of the synthesized Ag NPs and Ag/Zn BMNPs are presented as follows. Figure 4.2 (a-c) depicted that the absorption spectra, transmittance spectrum and energy bandgap for Ag NPs. Figure 4.3 (a-c) below depicted the absorption spectra, transmittance spectrum and energy bandgap for Ag/Zn BMNPs respectively.

The graph for the ultraviolet-visible absorption spectra sketch was from the raw data found from UV-Vis spectrophotometer as absorbance observed concerning different wavelength and the plot shown in figure 4.2-4.3 (a). The bandgap energy for the synthesized nanoparticles was determined by the Tauc relations which are discussed in equation (2.6) and the plots were shown in figure 4.2-4.3 (c) which fitted with the calculated bandgap energy from the equation (2.7) using the maximum wavelength absorbance and tabulated in table 4.5 below.

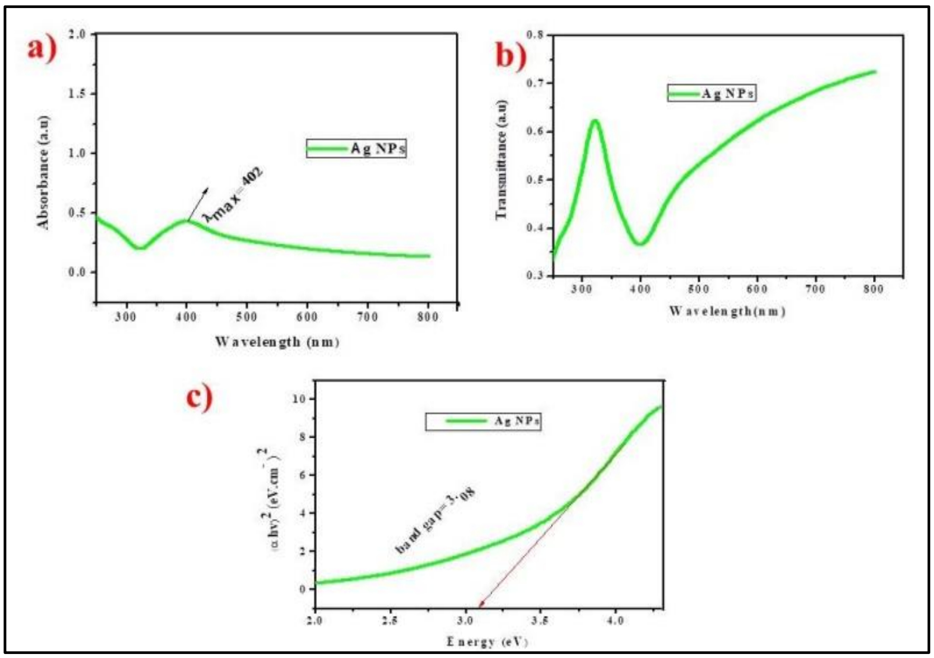

Figure 4.2: Wavelength versus Absorbance of Uv-vis spectroscopy, (b) wavelength versus transmittance (c) energy bandgap of Ag NPs

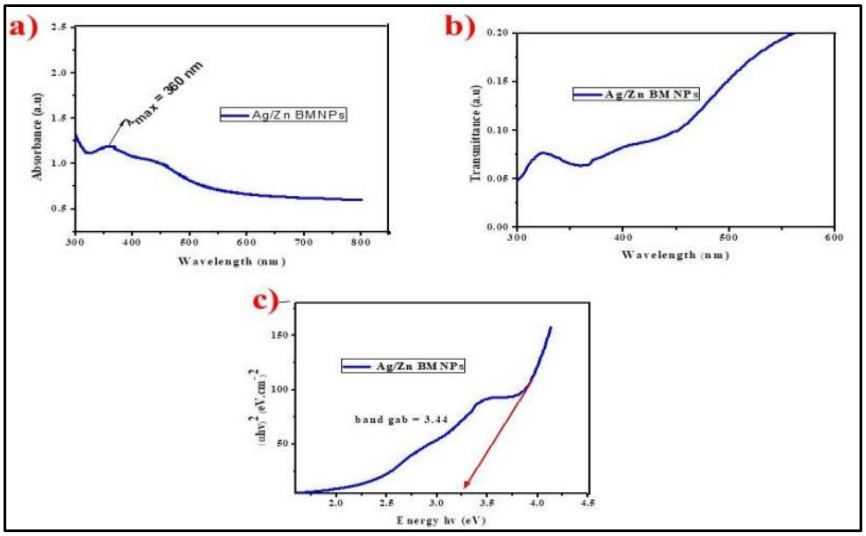

Figure 4.3: Wavelength versus Absorbance of Uv-vis spectroscopy, (b) wavelength versus transmittance (c) energy bandgap of Ag/Zn BMNPs.

Table 4.5: Calculated bandgap for Ag NPs and Ag/Zn BMNPs

Sample	λ_{max} (nm)	The bandgap (eV)
Ag NPs	402	3.08
Ag/Zn BMNPs	360	3.44

The maximum wavelength absorption peaks are seen at 360 nm and 402 nm for Ag/Zn BMNPs and Ag NPs, respectively. The corresponding optical band gap energy calculated using equation (2.7) was found to be 3.44 eV and 3.08 eV for Ag/Zn BMNPs and Ag NPs, respectively. As the report by Taran *et al*., showed the Uv-vis spectra for Ag NPs have 400 nm to 450 nm (Taran *et al*., 2016). Thus, the result obtained from the Uv-vis spectroscopy confirms that the synthesized NPs are Ag NPs.

The absorbance and the transmittance of Uv-vis spectroscopy of the sample are shown inverse relationships; which means as absorbance of the sample increases the transmittance is decreased. The graph above (figure 4.2-4.3) (a-b) confirms that as the absorbance increases the transmittance decreases. From the bandgap energy graph; as the bandgap energy decreases the particle size of nanoparticles decreases and the properties of nanoparticles are enhanced. For the band energy, the estimated Ag NPs particle size is lower than Ag/Zn BMNPs. Thus, the Ag NPs have enhanced properties than Ag/Zn BMNPs.

4.4. Scanning Electron Microscopy (SEM) analysis

The morphology and texture of the synthesized Ag NPs and Ag/Zn BMNPs were studied using SEM images. Figure 4.5 (a-b) shows the morphology of Ag NPs and Ag/Zn BMNPs respectively. The micrographs show that the NPs were found to possess spherical as well as irregular geometries. As the report by Perera *et al*., confirms the result wich obtained from the SEM is spherical (Perera *et al*., 2020).

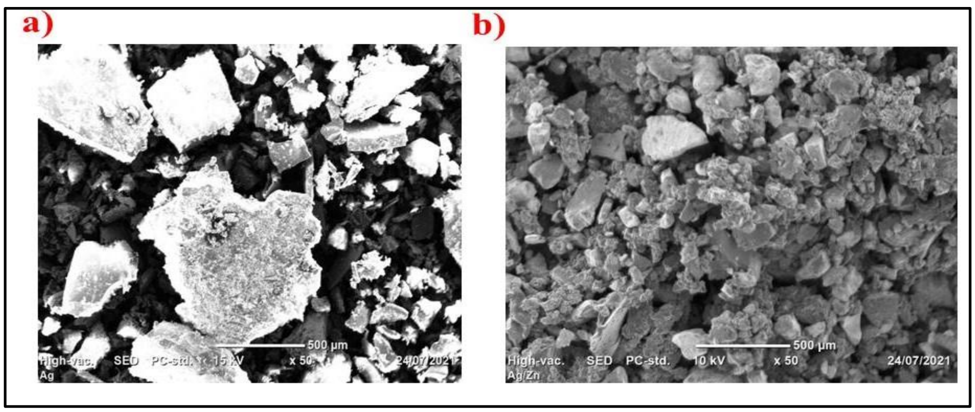

Figure 4.4: The SEM image of Ag NPs and Ag/Zn BMNPs

4.5. Fourier Transform Infra-Red (FT-IR) Analysis

The FT-IR spectra of synthesized Ag NPs and Ag/Zn BMNPs were recorded at room temperature in the range of 400 cm^{-1} to 4000 cm^{-1} with the resolution of 4 cm^{-1} using the KBr pellets. The absorption peaks were observed at 3426 cm^{-1}, 2923 cm^{-1}, 1635 cm^{-1}, 1384 cm^{-1}, 1053 cm^{-1} and 555 cm^{-1} with some small shifts for the synthesized Ag NPs and Ag/Zn BMNPs as shown in Figure 4.6. The broadband located at 3426 cm^{-1} for synthesized nanoparticles is due to O-H stretching vibration mode. The peak at Table 4.6 showed the functional group determined by FT-IR.

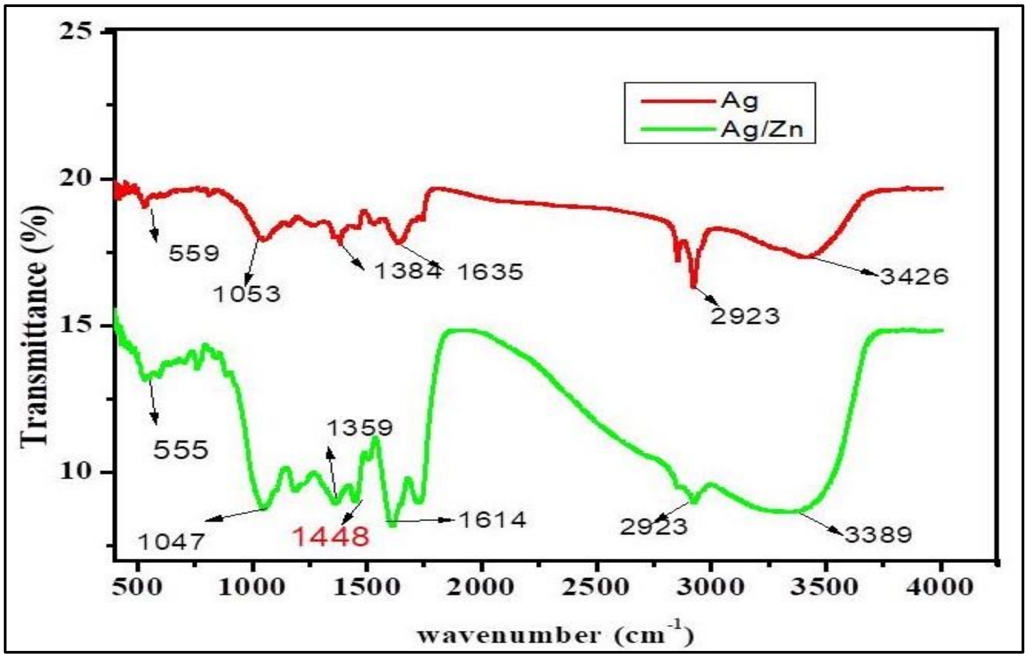

Figure 4.5: FT-IR spectra of synthesized of Ag NPs and Ag/Zn BMNPs

For Ag/Zn BMNPs there another additional absorption peak was observed at 1448 cm^{-1}. This additional spectrum showed metal-metal bond vibration frequency for Ag-Zn. As Heneczkowski *et al*., the report indicates the peak at 2923 cm^{-1} depicted the aromatic CH_3 for flavonoids (Heneczkowski *et al*., 2001), by the report of Ricci *et al*., the carbonyl stretching peaks at 1635 cm^{-1} showed the tannins functional group (Ricci *et al*., 2015). Khan et al., report that the peak at 1384 cm^{-1} showed the terpenoids (Khan *et al*., 2016). The peak at 3426 cm^{-1} showed the O-H stretching of phenolic groups as reported by Lakshmi, *et al*., (Lakshmi, *et al*., 2015). The synthesized nanoparticles were compared from Figure 4.6 the Ag/Zn BMNPs show small peak shifts. This means that the properties of Ag/Zn BMNPs are different from the individual synthesized Ag NPs

Table 4.6: The characteristic of FT-IR for Ag NPs and Ag/Zn BMNPs functional groups

Wavenumber (cm^{-1})	Functional group	Compound class	Intensity
3426	O-H stretching	Alcohol	Broad
2923	C-H stretching	Alkane	Medium
1635	C=C stretching	Aromatic	Strong
1384	C-H bend	Alkane	Weak
1053	C-O	Aliphatic amine	Strong
555	C-X	Halo alkane	Weak

4.6. Antibacterial Activity Studies

In this section, the antibacterial activities of the synthesized NPs were discussed. Figure 4.7 (a-d) indicates the suspensions of distinct concentrations synthesized Ag NPs and Ag/Zn BMNPs towards the gram-negative bacteria species, *E. coli* and *P. aeruginosa* and gram-positive species, *S. pyogenes* and *S. aureus*, respectively which were determined by the agar disc diffusion assay

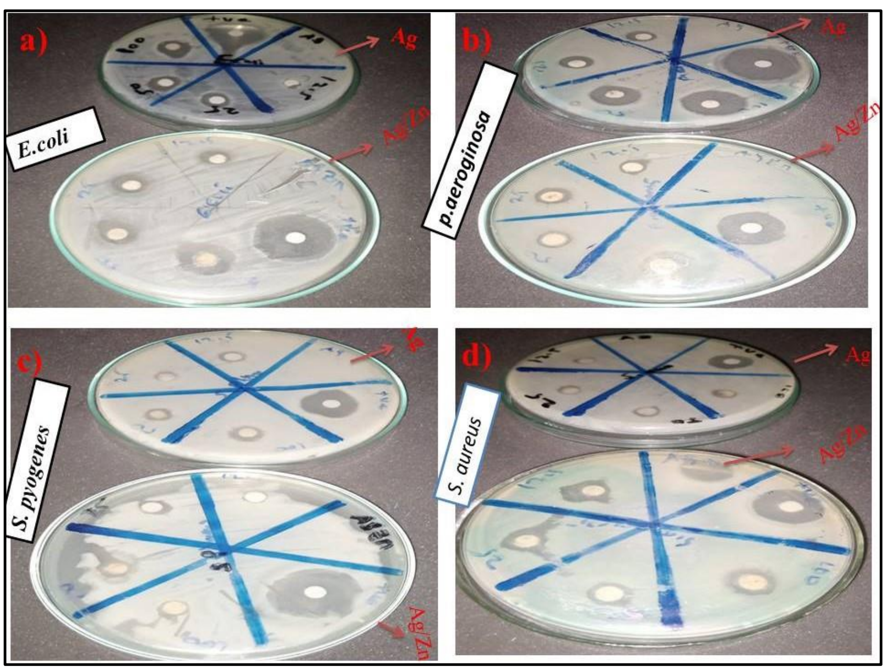

Figure 4.6: Antibacterial activities of Ag NPs and Ag/Zn BMNPs against (a) *E. coli*, (b) *P. aeruginosa*, (c) *S. pyogenes* and (d) *S. aureus*

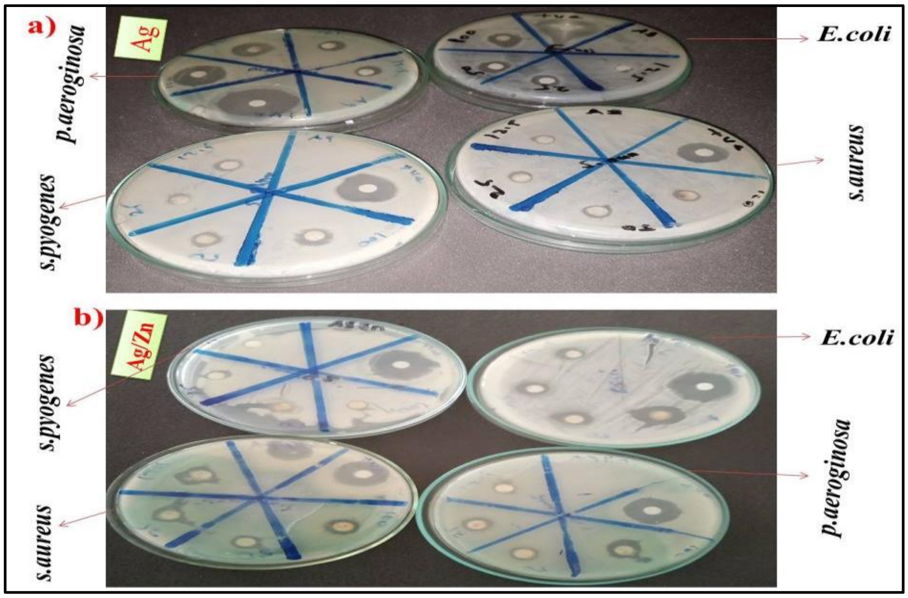

Figure 4.7: The inhibition zone of (a) Ag NPs and (b) Ag/Zn BMNPs against *E.coli*, *P. aeruginosa*, *S. pyogenes* and *S. aureus*

The antibacterial activity of the synthesized Ag NPs and Ag/Zn BMNPs against the bacterial strains gram-negative *E.coli* and *P. aeruginos* and gram-positive *S. pyogenes* and *S. aureus* were tabulated and discussed in the tables (4.6 and 4.7) respectively. The presence of an inhibition zone indicates that the mechanism of the biocidal action of synthesized nanoparticles involves disruption of the cell membrane of bacterial species and finally leads to the death of pathogens. Thus, the size of the inhibition zone was different according to the type of pathogens, the concentration of the synthesized NPs and the type of NPs.

In our study, the gram-negative bacteria for Ag NPs and Ag/Zn BMNPs has more susceptibility to nanoparticle-mediated toxicity as compared to gram-positive bacteria for Ag NPs and Ag/Zn BMNPs as shown in figure 4.8 (a-b) below respectively, because gram-negative bacteria have a thin layer of peptidoglycan as compared to gram-positive bacteria which exhibits less resistance on nanoparticle interaction with the cell membrane of gram-negative bacteria. Therefore, cell wall thickness, structure, and composition play an important role in nanoparticle interaction with bacteria.

Table 4.7: Zones of inhibition of Ag NPs and Ceftriaxone (+ve control) with different concentrations against different bacterial strains

Sample	Concentration (μg/ml)	Zone of inhibition (mm)			
		Gram-negative species		Gram-positive species	
		E.coli	*P. aeruginosa*	*S.pyogenes*	*S.aureus*
Ag NPs	100.0	18.50 ±0.87	19±1.32	17.83±3.25	10.27 ± 1.50
	50.0	13.83±1.04	16± 1.00	9.33± 0.76	8.23 ± 0.06
	25.0	10.8±1.15	12± 1.50	7.67± 1.15	7 ± 0.44
	12.5	7.4±0.60	9.17± 2.56	6.77± 0.25	6.6 ± 0.40
Ceftriaxone (+ve cont)	30.0	25± 1.80	25.67± 4.31	25.17± 2.02	19.63 ± 2.27

Table 4.8: Zone of inhibition of Ag/Zn BMNPs and Ceftriaxone (+ve cont) against different bacterial species with different concentration

Sample	Concentration (μg/ml)	Zone of inhibition (mm)			
		Gram-negative species		Gram-positive species	
		E.coli	*P. aeruginosa*	*S.pyogenes*	*S.aureus*
Ag/Zn BMNPs	100.0	13 ± 1.74	16.5 ± 0.87	8.97 ± 0.56	12 ± 1.04
	50.0	11.1 ± 0.98	11.67 ± 2.31	7.83 ± 0.25	9.43 ± 1.01
	25.0	9.5 ± 0.20	8.33 ± 0.29	7.03 ± 0.21	7.83 ± 0.40
	12.5	8.63 ± 0.51	7 ± 0.30	6.7 ± 0.17	6.93 ± 0.93
Ceftriaxone (+ve cont)	30.0	20.25 ± 3.02	24 ± 1.0	20.37 ± 1.30	18.53 ± 0.29

Where: *E.coli* is *Escherichia coli*, *P. aeruginosa* is *Pseudomonas aeruginosa*, *S.pyogenes* is *Streptococcus pyogenes* and *S.aureus* is *Staphylococcus aureus*

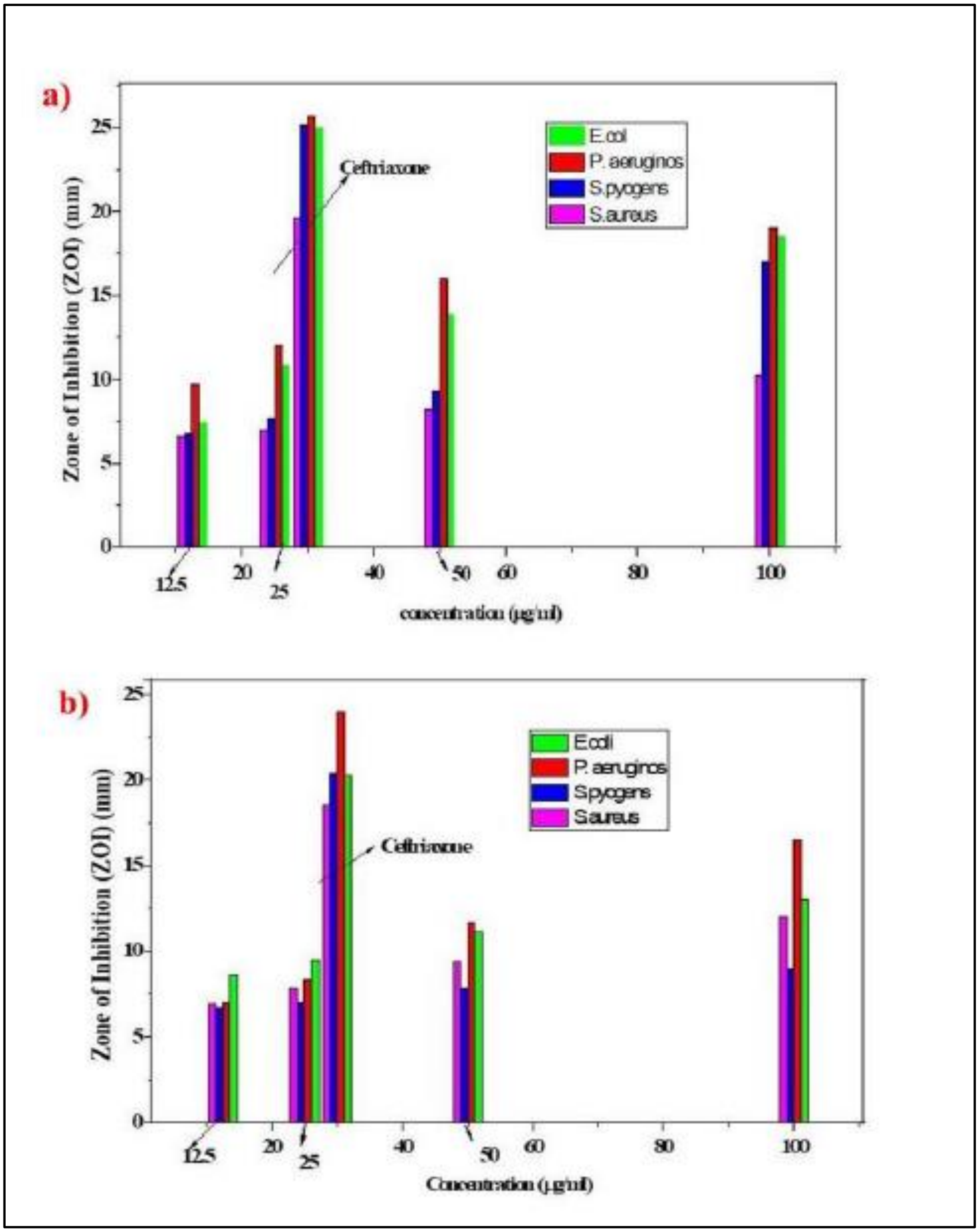

Figure 4.8: The zone of inhibition of (a) Ag NPs, (b) Ag/Zn BMNPs and Ceftriaxone (+ve cont) against bacterial strains gram negative, *E.coli* and *P. aeruginosa* and gram positive, *S. pyogenes* and *S.aureus*.

When the synthesized NPs were compared for the synthesized Ag NPs and Ag/Zn BMNPs activities against selected bacterial strains (*E.coli*, *P. aeruginosa*, *S pyogenes* and *S.aureus)* the Ag NPs exhibited best inhibition activities toward the selected bacterial species than that of Ag/Zn BMNPs inhibition activities. Figure 4.9 (a-d) shows that the inhibition activities of Ag NPs and Ag/Zn BMNPs against (a) *E.coli*, (b) *P. aeruginosa*, (c) *S pyogenes* and (d) *S.aureus* respectively.

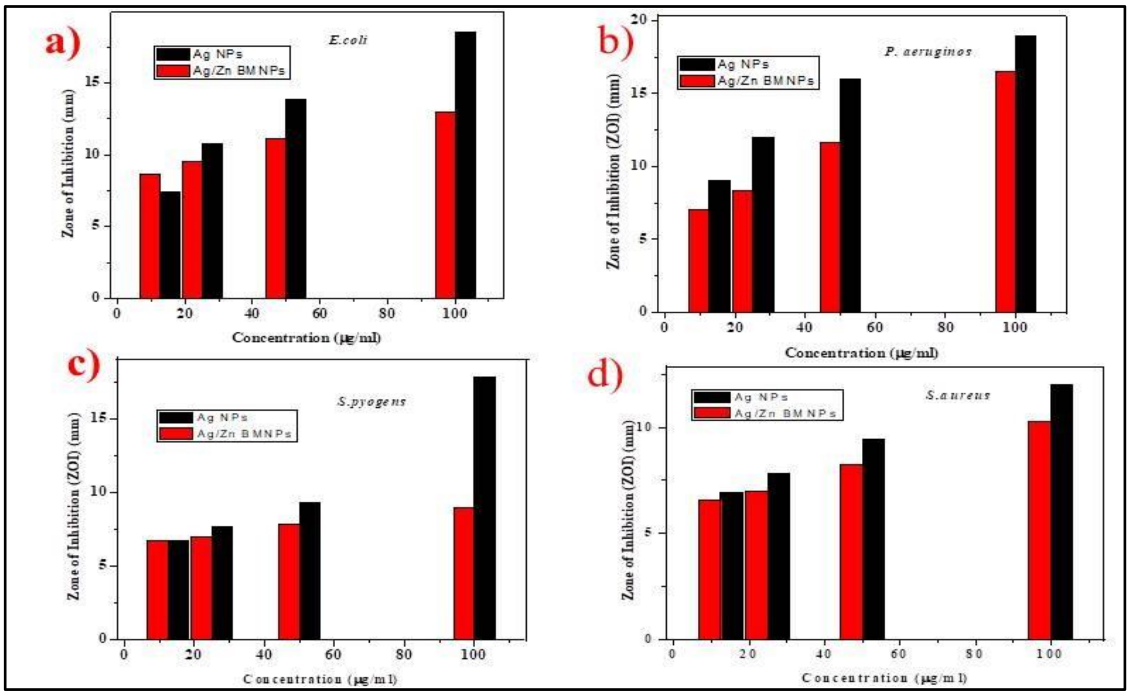

Figure 4.9: The inhibition activities of Ag NPs and Ag/Zn BMNPs against *E.coli*, *P. aeruginosa*, *S pyogenes* and *S.aureus*

5. CONCLUSIONS AND RECOMMENDATIONS

5.1. Conclusions

The Ag NPs and Ag/Zn BMNPs were synthesized via the green synthesis method by using garlic plant extract. The synthesized NPs were then characterized by XRD, UV-Vis, SEM, and FT-IR Spectroscopy. The XRD result confirmed the cubic crystal structure for both Ag NPs and Ag/Zn BMNPs with average particle sizes of 9.31 nm and 17.47 nm respectively. The maximum absorption wavelengths were recorded at 360 nm and 402 nm for Ag/Zn BMNPs and Ag NPs. The energy bandgap values for Ag/Zn BMNPs and Ag NPs were found to be, 3.44 eV and 3.08 eV, respectively. The nearly spherical morphology of synthesized NPs was confirmed by SEM micrographs. The surface bonding features were confirmed by FT-IR analysis. The antibacterial studies of synthesized Ag/Zn BMNPs and Ag NPs conducted against the gram-negative species, *E. coli* and *P. aeruginosa* and gram-positive species, *S. pyogenes* and *S. aureus* revealed more efficiency for Ag NPs. On the other hand, as particle size becomes lower the NPs have the enhanced properties; thus, Ag NPs have lower particle size than Ag/Zn BMNPs. So, the Ag NPs have a greater zone of inhibition than that of Ag/Zn BMNPs.

5.2. Recommendations

Bimetallic nanoparticle synthesis through green methods is one of the emerging research areas with huge future prospective. Thus, further studies may be required for the synthesis of Ag/Zn BMNPs and their applications such as in the field of optoelectronic devices, catalysis and biomedical applications.

Research Fund Acknowledgment

This work is financially supported by Adama Science and Technology University and the Ministry of Innovation and Technology of Ethiopia under the grant number **ASTU/SMR/253/21**, Adama, Ethiopia.

6. REFERENCE

Alahmad, A., Feldhoff, A., Bigall, N. C., Rusch, P., Scheper, T., & Walter, J. G. (2021). Hypericum perforatum L.-mediated green synthesis of silver nanoparticles exhibiting antioxidant and anticancer activities. *Nanomaterials*, *11*(2), 487.

Al-Haddad, J., Alzaabi, F., Pal, P., Rambabu, K., & Banat, F. (2020). Green synthesis of bimetallic copper–silver nanoparticles and their application in catalytic and antibacterial activities. *Clean Technologies and Environmental Policy*, *22*(1), 269-277.

Arora, N., Thangavelu, K., & Karanikolos, G. N. (2020). Bimetallic nanoparticles for antimicrobial applications. *Frontiers in Chemistry*, *8*, 412.

Atomssa, T., & Gholap, A. V. (2011). Characterization of caffeine and determination of caffeine in tea leaves using uv-visible spectrometer. *African Journal of Pure and Applied Chemistry*, *5*(1), 1-8.

Ayalew, A. (2015). Evaluation of garlic (Allium sativum L.) varieties for bulb yield and growth at dabat, northwestern Ethiopia. *Open Access Library Journal*, *2*(01), 1.

Bang, J. H., & Suslick, K. S. (2010). Applications of ultrasound to the synthesis of nanostructured materials. *Advanced materials*, *22*(10), 1039-1059.

Basavegowda, N., Mandal, T. K., & Baek, K. H. (2020). Bimetallic and trimetallic nanoparticles for active food packaging applications: A review. *Food and Bioprocess Technology*, *13*(1), 30-44.

Bhatt, R., & Gupta, S. (2018). Nano Particles and Their Mode of Action in Environment. In *Microbial Biotechnology in Environmental Monitoring and Cleanup* (pp. 212-219). IGI Globa.

Chalie-u, R., Jakhar, S. R., Mitra, N. G., Wasnikar, A. R., & Sahu, R. K. (2019). Biomass Production of *Trichoderma viride* as Influenced by Carbon and Nitrogen Sources. *International Journal of Current Microbiology and Applied Sciences*, *8*(6), 3269-3274.

Chauhan, J., & Yadav, S. (2018). Synthesis and Characterization of Bimetallic Nanoparticles by 2-Thiotic Acid for Selective Growth of SWCNT. *International Journal of Applied Nanotechnology*, *4*(2), 48-58.

Cullity. B.D and Stock S.R. (2001). Elements of X-ray Diffraction. Prentice Hall, Upper Saddle River, NJ, 5(3), 20-31.

De Jong, W. H., & Borm, P. J. (2008). Drug delivery and nanoparticles: applications and hazards. *International journal of nanomedicine*, *3*(2), 133.

De León-Quiroz, E. L., García-Cerda, L. A., Obregón, D. V., Pedraza, A. P., Larios-Rodríguez, E., & José-Yacaman, M. (2012). Synthesis and characterization of alloys and bimetallic nanoparticles of CuNi prepared by Sol-Gel method. *MRS Online Proceedings Library*, *1479*(1), 9-14.

Dehghan Banadaki, A., & Kajbafvala, A. (2014). Recent advances in facile synthesis of bimetallic nanostructures: An overview. *Journal of Nanomaterials*, *2014*.

Dietrich, C., Chen, S., Uzunidis, G., Hähsler, M., Träutlein, Y., & Behrens, S. (2021). Bimetallic Pd/Sn-based Nanoparticles and their Catalytic Properties in the Semihydrogenation of Diphenylacetylene. *Chemistry Open*, *10*(2), 296.

Duan, S., & Wang, R. (2013). Bimetallic nanostructures with magnetic and noble metals and their physicochemical applications. *Progress in Natural Science: Materials International*, *23*(2), 113-126.

Esparza, R., Téllez-Vázquez, O., Ángeles-Pascual, A., & Pérez, R. (2015). Synthesis and characterization of bimetallic nanoparticles by cs-corrected scanning transmission electron microscopy. In *Materials Characterization* (pp. 35-42). Springer, Cham.

Firdhouse, M. J., & Lalitha, P. (2015). Biosynthesis of silver nanoparticles and its applications. *Journal of Nanotechnology*, *2015*.

Greish, K., Alqahtani, A. A., Alotaibi, A. F., Abdulla, A. M., Bukelly, A. T., Alsobyani, F. M., & Kamal, A. (2019). The effect of silver nanoparticles on learning, memory and social interaction in BALB/C mice. *International journal of environmental* *research and public health*, *16*(1), 148.

Gude, R., Joshi, A. B., Bhandarkar, A., Shirodker, A., & Bhangle, S. (2016). Synthesis and characterization of silver nanoparticles from the roots of Aphanamixis polystachya. *World Jour of Pharm Research*, *2*(5), 1399-408.

Gul, R., Jan, S. U., Faridullah, S., Sherani, S., & Jahan, N. (2017). Preliminary phytochemical screening, quantitative analysis of alkaloids, and antioxidant activity of crude plant extracts from Ephedra intermedia indigenous to Balochistan. *The Scientific World Journal*, *2017*.

Gupta, S., Hemlata, H., & Tejavath, K. (2020). Synthesis, characterization and comparative anticancer potential of phytosynthesized mono and bimetallic nanoparticles using Moringa oleifera aqueous leaf extract. *Beilstein Arch*, *1*, 95.

Hai, Z., Kolli, N. E., Chen, J., & Remita, H. (2014). Radiolytic synthesis of Au–Cu bimetallic nanoparticles supported on TiO 2: application in photocatalysis. *New Journal of Chemistry*, *38*(11), 5279-5286.

Haider, A., & Kang, I. K. (2015). Preparation of silver nanoparticles and their industrial and biomedical applications: a comprehensive review. *Advances in materials science and engineering*, *2015*.

Heneczkowski, M., Kopacz, M., Nowak, D., & Kužniar, A. (2001). "Department of Polymer Technology,"Department of Inorganic and Analytical Chemistry, Faculty of Chemistry, Rzeszów University of Technology. *Acta Poloniae Pharmaceutica*, *58*(6), 415-420.

Hjältén, A., Germann, M., Krzempek, K., Hudzikowski, A., Głuszek, A., Tomaszewska, D., & Foltynowicz, A. (2021). Optical frequency comb Fourier transform spectroscopy of 14N216O at 7.8 µm. *Journal of Quantitative Spectroscopy and Radiative Transfer*, *271*, 107734.

Huynh, K. H., Pham, X. H., Kim, J., Lee, S. H., Chang, H., Rho, W. Y., & Jun, B. H.

(2020). Synthesis, properties, and biological applications of metallic alloy nanoparticles. *International Journal of Molecular Sciences*, *21*(14), 5174.

Jassal, K. (2020). *Nanotechnology Mediated Enhancement in Engineering Nanotechnology Mediated Enhancement in Engineering*. *10*(September), 12881–12888.

Jha, A. K., & Prasad, K. (2010). Green synthesis of silver nanoparticles using Cycas leaf. *International Journal of Green Nanotechnology: Physics and Chemistry*, *1*(2), P110-P117.

Jubu, P. R., Yam, F. K., Igba, V. M., & Beh, K. P. (2020). Tauc-plot scale and extrapolation effect on bandgap estimation from UV–vis–NIR data–a case study of β-Ga2O3. *Journal of Solid State Chemistry*, *290*, 121576.

Kalpana, V. N., & Devi Rajeswari, V. (2018). A review on green synthesis, biomedical applications, and toxicity studies of ZnO NPs. *Bioinorganic chemistry and applications*, *2018*.

Karnib, M., Holail, H., Olama, Z., Kabbani, A., & Hines, M. (2013). Original Research Article The Antibacterial Activity of Activated Carbon, Silver, Silver Impregnated Activated Carbon and Silica Sand Nanoparticles against Pathogenic E. coli BL21. *Int. J. Curr. Microbiol. App. Sci*, *2*(4), 20-30.

Kasim, M., Ann, O., & Yahaya, M. M. (2019). Larvicidal activity of garlic (Allium sativum) on Anopheles and Culex mosquito larvae. *Pharmacology Online*, *2*, 130-138.

Khan, M. A., Khan, T., & Nadhman, A. (2016). Applications of plant terpenoids in the synthesis of colloidal silver nanoparticles. *Advances in colloid and interface science*, *234*, 132-141.

Khatami, M., Alijani, H. Q., & Sharifi, I. (2018). Biosynthesis of bimetallic and core–shell nanoparticles: their biomedical applications–a review. *IET nanobiotechnology*, *12*(7), 879-887.

Khatami, M., Alijani, H. Q., & Sharifi, I. (2018). Biosynthesis of bimetallic and core–shell nanoparticles: their biomedical applications–a review. *IET nanobiotechnology*, *12*(7), 879-887.

Kumar, K. K. P., Dinesh, N. D., & Murari, S. K. (2019). Synthesis of CuO and Ag doped CuO nanoparticles from Muntingia calabura leaf extract and evaluation of their antimicrobial potential. *International Journal of Nano and Biomaterials*, *8*(3-4), 228-252.

Kumar, T. S. J., Balavigneswaran, C. K., Packiaraj, R. M., Veeraraj, A., Prakash, S., Hassan, Y. N., & Srinivasakumar, K. P. (2013). Green Synthesis of Silver Nanoparticles by Plumbago indica and Its Antitumor Activity against Dalton's Lymphoma Ascites Model. *BioNanoScience*, *3*(4), 394-402.

Lakshmi, N. D. M., Mahitha, B., Madhavi, T., & Sushma, N. J. (2015). Phytochemical screening and FTIR analysis of Clitoria ternatea leaves. *International Journal of Scientific & Engineering Research*, *6*(2), 287-290.

Lemilemu, F., Girmay, S., Shenkute, K., & Endale, M. (2020). Antibacterial steroids from roots of Bersama abyssinica. *Ethiopian Journal of Sciences and Sustainable Development*, *7*(1), 27-34.

Li, Z., Huang, H., Shang, T., Yang, F., Zheng, W., Wang, C., & Manohar, S. K. (2006). Facile synthesis of single-crystal and controllable sized silver nanoparticles on the surfaces of polyacrylonitrile nanofibres. *Nanotechnology*, *17*(3), 917.

Mandal, D., Bolander, M. E., Mukhopadhyay, D., Sarkar, G., & Mukherjee, P. (2006). The use of microorganisms for the formation of metal nanoparticles and their application. *Applied microbiology and biotechnology*, *69*(5), 485-492.

Mazhar, T., Shrivastava, V., & Tomar, R. S. (2017). Green synthesis of bimetallic nanoparticles and its applications: a review. *Journal of Pharmaceutical Sciences and Research*, *9*(2), 102.

Mohamad, N. A. N., Jai, J., Arham, N. A., & Hadi, A. (2013). A short review on the synthesis of bimetallic nanoparticles using plant extract. In *2013 IEEE international conference on control system, computing and engineering*, 334-339.

Murthy, H. A., Zeleke, T. D., Ravikumar, C. R., Kumar, M. A., & Nagaswarupa, H. P. (2020). Electrochemical properties of biogenic silver nanoparticles synthesized using Hagenia abyssinica (Brace) JF. Gmel. Medicinal plant leaf extract. *Materials Research Express*, *7*(5), 055016.

Nadaroglu, H., Güngör, A. A., & Selvi, İ. N. C. E. (2017). Synthesis of nanoparticles by green synthesis method. *International Journal of Innovative Research and Reviews*, *1*(1), 6-9.

Nadeem, A., Naz, S., Ali, J. S., Mannan, A., & Zia, M. (2019). Synthesis, characterization and biological activities of monometallic and bimetallic nanoparticles using Mirabilis jalapa leaf extract. *Biotechnology Reports*, *22*, e00338.

Natsuki, J., Natsuki, T., & Hashimoto, Y. (2015). A review of silver nanoparticles: synthesis methods, properties and applications. *Int. J. Mater. Sci. Appl*, *4*(5), 325-332.

Nazeruddin, G. M., Prasad, R. N., Shaikh, Y. I., & Shaikh, A. A. (2014). Synergetic effect of Ag-Cu bimetallic nanoparticles on antimicrobial activity. *Der Pharmacia Lettre*, *3*, 129-36.

Netoa, A. A. T., Faceto, B., & Bueno, C. M. (2013). *Characterization of Au /(Ag or Pd) Bimetallic Nanoparticles Supported on SBA-15*. 12521.

Ovais, M., Khalil, A. T., Islam, N. U., Ahmad, I., Ayaz, M., Saravanan, M., ... & Mukherjee, S. (2018). Role of plant phytochemicals and microbial enzymes in biosynthesis of metallic nanoparticles. *Applied microbiology and biotechnology*, *102*(16), 6799-6814.

Patra, N., Taviti, A. C., Sahoo, A., Pal, A., Beuria, T. K., Behera, A., & Patra, S. (2017). Green synthesis of multi-metallic nanocubes. *RSC advances*, *7*(56), 35111-35118.

Perera, K. M. K. G., Kuruppu, K. A. S. S., Chamara, A. M. R., & Thiripuranathar, G.

(2020). Characterization of spherical Ag nanoparticles synthesized from the agricultural wastes of Garcinia mangostana and Nephelium lappaceum and their applications as a photo catalyzer and fluorescence quencher. *SN Applied Sciences*, *2*(12), 1-24.

Prem Nawaz, M., Raja Mohamed, S., & Mohamed Rafi, K. (2018). Green synthesis of Ag NPs synthesized by using Cassia auriculata leaves (C.auriculata) and its applications of cancer activity. *IOSR Journal Of Pharmacy Www.Iosrphr.Org*, *8*(7), 39–44.

Ricci, A., Olejar, K. J., Parpinello, G. P., Kilmartin, P. A., & Versari, A. (2015). Application of Fourier transforms infrared (FTIR) spectroscopy in the characterization of tannins. *Applied Spectroscopy Reviews*, *50*(5), 407-442.

Rodriguez, J. A., & Goodman, D. W. (1992). The nature of the metal-metal bond in bimetallic surfaces. *Science*, *257*(5072), 897-903.

Rostek, A., Loza, K., Heggen, M., & Epple, M. (2019). X-ray powder diffraction to analyse bimetallic core–shell nanoparticles (gold and palladium; 7–8 nm). *RSC advances*, *9*(46), 26628-26636.

Salunke, B. K., Shin, J., Sawant, S. S., Alkotaini, B., Lee, S., & Kim, B. S. (2014). Rapid biological synthesis of silver nanoparticles using Kalopanax pictus plant extract and their antimicrobial activity. *Korean Journal of Chemical Engineering*, *31*(11), 2035-2040.

Shah, A., Qureshi, R., Khan, S. B., Asiri, A. M., Shah, A. U. H. A., Ishaq, M., ... & Zia, M. A. (2015). Spectroscopic analysis of Au-Cu alloy nanoparticles of various compositions synthesized by a chemical reduction method. *Advances in Materials Science and Engineering*, *2015*.

Sharma, G., Alothman, Z. A., Kumar, A., Sharma, S., Ponnusamy, S. K., & Naushad, M. (2017). Fabrication and characterization of a nanocomposite hydrogel for combined photocatalytic degradation of a mixture of malachite green and fast green dye. *Nanotechnology for Environmental Engineering*, *2*(1), 4.

Sharma, G., Kumar, A., Sharma, S., Naushad, M., Dwivedi, R. P., ALOthman, Z. A., & Mola, G. T. (2019). Novel development of nanoparticles to bimetallic nanoparticles and their composites: a review. *Journal of King Saud University-Science*, *31*(2), 257-269.

Sintubin, L., Verstraete, W., & Boon, N. (2012). Biologically produced nanosilver: current state and future perspectives. *Biotechnology and Bioengineering*, *109*(10), 2422-2436.

Slocik, J. M., & Naik, R. R. (2006). Biologically programmed synthesis of bimetallic nanostructures. *Advanced Materials*, *18*(15), 1988-1992.

Sorbiun, M., Shayegan Mehr, E., Ramazani, A., & Mashhadi Malekzadeh, A. (2018). Biosynthesis of metallic nanoparticles using plant extracts and evaluation of their antibacterial properties. *Nanochemistry Research*, *3*(1), 1-16.

Srinoi, P., Chen, Y. T., Vittur, V., Marquez, M. D., & Lee, T. R. (2018). Bimetallic nanoparticles: enhanced magnetic and optical properties for emerging biological applications. *Applied Sciences*, *8*(7), 1106.

Su, Y. H., & Wang, W. L. (2013). Surface plasmon resonance of Au-Cu bimetallic nanoparticles predicted by a quasi-chemical model. *Nanoscale research letters*, *8*(1), 1-6.

Švecová, M., Ulbrich, P., Dendisová, M., & Matějka, P. (2018). SERS study of riboflavin on green-synthesized silver nanoparticles prepared by reduction using different flavonoids: What is the role of flavonoid used. *Spectrochimica Acta Part A: Molecular and Biomolecular Spectroscopy*, *195*, 236-245.

Sylvestre, J. P., Poulin, S., Kabashin, A. V., Sacher, E., Meunier, M., & Luong, J. H. (2004). Surface chemistry of gold nanoparticles produced by laser ablation in aqueous media. *The Journal of Physical Chemistry B*, *108*(43), 16864-16869.

Taran, M., Rad, M., & Alavi, M. (2016). Characterization of Ag nanoparticles biosynthesized by Bacillus sp. HAI4 in different conditions and their antibacterial effects. *J Appl Pharm Sci*, *6*(11), 094-099.

Thirumurugan, A., Jiflin, G. J., Rajagomathi, G., Tomy, N. A., Ramachandran, S., & Jaiganesh, R. (2010). Biotechnological synthesis of gold nanoparticles of Azadirachta indica leaf extract. *Int J Biol Technol*, *1*(1), 75-7.

Tian, Y., Orlu, M., Woerdenbag, H. J., Scarpa, M., Kiefer, O., Kottke, D., ... & Visser, J. C. (2019). Oromucosal films: From patient centricity to production by printing techniques. *Expert opinion on drug delivery*, *16*(9), 981-993.

Tiwari, P., Das, G. M., & Dantham, V. R. (2020). Optical Properties of Au-Ag Bimetallic Nanoparticles of Different Shapes for Making Efficient Bimetallic-Photonic Whispering Gallery Mode Hybrid Microresonators. *Plasmonics*, *15*(5), 1251-1260.

Toshima, N., & Yonezawa, T. (1998). Bimetallic nanoparticles-novel materials for chemical and physical applications. *New Journal of Chemistry*, *22*(11), 1179-1201.

Tran, Q. H., & Le, A. T. (2018). Corrigendum: Silver nanoparticles: synthesis, properties, toxicology, applications and perspectives (Adv. Nat. Sci: Nanosci. Nanotechnol. 4 033001). *Advances in Natural Sciences: Nanoscience and Nanotechnology*, *9*(4), 049501.

Tyagi, S., Chirag, P. J., Poonam, D., Dhruv, M., Ishita, S., Labu, Z. K., ... & Patel, K. N. (2013). Importance of garlic (Allium Sativum): an exhaustive review. *Journal of Drug Discovery and Therapeutics*, *1*(4), 23-27.

Van Tien, H., Tri, N., Anh, N. P., Nhi, D. M., Bich, L. T., Hang, D. N. L., & Van Minh, N. (2020). Characterization and Antibacterial Activity of Silver-Manganese Bimetallic Nanoparticles Biofabricated Using Arachis Pintoi Extract. *International Journal of Pharmaceutical and Phytopharmacological Research (eIJPPR)*, *10*(1), 70-76.

Venkatesh, N., Bhowmik, H., & Kuila, A. (2018). Metallic nanoparticle: a review. *Biomedical Journal of Scientific & Technical Research*, *4*(2), 3765-3775.

Vorokh, A. S. (2018). Scherrer formula: estimation of error in determining small nanoparticle size. *Nanosystems: Physics, Chemistry, Mathematics*, *9*(3), 364–369.

Wu, M. L., Chen, D. H., & Huang, T. C. (2001). Synthesis of Au/Pd bimetallic nanoparticles in reverse micelles. *Langmuir*, *17*(13), 3877-3883.

Zaib, S., & Iqbal, J. (2019). Nanotechnology: Applications, techniques, approaches, & the advancement in toxicology and environmental impact of engineered nanomaterials. *Importance & Applications of Nanotechnology*, 8.

Zaleska-Medynska, A., Marchelek, M., Diak, M., & Grabowska, E. (2016). Noble metal-based bimetallic nanoparticles: the effect of the structure on the optical, catalytic and photocatalytic properties. *Advances in colloid and interface science*, *229*, 80-107.